DEVELOPMENT OF CANCER THERAPHY WITH ICG-PDT SUPPORTED BY GOLD NANOPARTICLES

by

Sena SALTA SAVAŞ

BSc., in Biomedical Engineering, Yeditepe University, 2015

Submitted to the Institute of Biomedical Engineering
in partial fulfillment of the requirements
for the degree of
Master of Science
in
Biomedical Engineering

Boğaziçi University
2019

DEVELOPMENT OF CANCER THERAPHY WITH ICG-PDT SUPPORTED BY GOLD NANOPARTICLES

APPROVED BY:

Prof. Dr. Murat Gülsoy .....
(Thesis Advisor)

Assist. Prof. Dr. Duygu Ege .....

Assist. Prof. Dr. Hakan Solmaz .....

DATE OF APPROVAL:

ACKNOWLEDGMENTS

First and foremost, I would like to express my sincerest gratitude to my thesis supervisor, Prof. Murat Gülsoy, for his patient guidance throughout my thesis. This thesis would not have been completed without his guidance, immense knowledge and encouragement.

I would also like to acknowledge Assoc. Prof. Bora Garipcan for his valuable help and insightful comments. Besides, I would like to express my thanks to his group members for sharing their lab opportunities.

During my experimental work, I have been endowed with the invaluable guidance and help of Melike Güney Akkurt and Dr. Mustafa Kemal Ruhi. I also owe my friends in the Biophotonics laboratory many thanks for their support.

Last but not least, I am especially indebted to my parents Fatma and İsmail Salta for their love and support throughout my life and my education. And to my dear husband Emin, thank you for being by my side through this period, as you are through everything.

ACADEMIC ETHICS AND INTEGRITY STATEMENT

I, Sena Salta Savaş, hereby certify that I am aware of the Academic Ethics and Integrity Policy issued by the Council of Higher Education (YÖK) and I fully acknowledge all the consequences due to its violation by plagiarism or any other way.

Name :

Signature:

Date:

ABSTRACT

DEVELOPMENT OF CANCER THERAPHY WITH ICG-PDT SUPPORTED BY GOLD NANOPARTICLES

Photodynamic therapy (PDT) is an application based on the killing of unwanted cells with photochemical reactions based on photosensitizer induced by light at an appropriate wavelength and the use of oxygen in the environment. Spherical gold nanoparticles (AuNPs) have been interesting because of their easy synthesis and easy functionalization thanks to their conjugation properties. The aim of this study is to investigate the efficacy of PDT on cancer cells with an 809-nm laser, which has higher optical penetration to biological tissues than other lasers using the indocyanine green (ICG) as a photosensitizer loaded onto a gold nanoscale carrier. For this purpose, PDT was applied to the cells of the prostate (PC-3) and colon (Caco-2) cancer and the results were compared with control groups and each other. Cell viability was monitored by MTT test to measure the efficacy of the dose of AuNP-ICG used during these experiments. On Caco-2 and PC-3 cell lines, 25 μM, 50 μM and 100 μM ICG concentrations and 25, 50 and 100 J/cm^2 laser power density groups were compared. As a result of these studies, it was found that the AuNP-ICG had a toxic effect on treated cell lines. It was also observed that colon cancer cells were more resistant to PDT with AuNP-ICG than prostate cancer cells. Although there was no significant decrease in cell viability without toxic effect in PC-3 cells, they showed a significant viability decrease compared to the control group. In Caco-2 cells, this significant decrease was observed at higher dosages and higher energy density.

Keywords: Photodynamic Therapy, Prostate Cancer, Colon Cancer, Indocyanine Green, Gold Nanoparticles.

ÖZET

ALTIN NANOPARÇACIK DESTEKLİ ISY-FDT İLE KANSER TEDAVİSİ GELİŞTİRİLMESİ

Fotodinamik terapi (FDT), uygun dalga boyunda ışık ile uyarılmış fotosensitizan ve ortamdaki oksijenin kullanılması ile oluşan fotokimyasal reaksiyonlar aracılığıyla istenmeyen hücrelerin öldürülmesine dayanan bir uygulamadır. Nanoyapılar içerisinde küresel altın nanoparçacık (AuNP) kolay sentezlenebilmesi ve konjugasyon özellikleri sayesinde kolay işlevselleştirilebilmesi ile ilgi çekici olmuştur. Bu çalışmada biyolojik dokulara optik girginliği diğer lazerlere kıyasla daha yüksek olan 809-nm lazer ile indosiyanin yeşilinin (ISY) altın nano taşıyıcıya yüklenerek kullanılması durumunda kanser hücreleri üzerinde oluşan FDT etkinliğinin incelenmesi amaçlanmaktadır. Bu amaçla prostat (PC-3) ve kolon (Caco-2) kanser tiplerine ait hücrelere altın nanoparçacıklara yüklenmiş ISY kullanılarak FDT uygulaması yapılmış ve sonuçlar kontrol grupları ve birbirleriyle karşılaştırılmıştır. Bu deneyler sırasında kullanılan ISY yüklü nanoparçacık dozunun etkinliğini ölçmek için hücre canlılığı MTT testi ile izlenmiştir. Caco-2 ve PC-3 hücre dizileri üzerinde, 25 μM, 50 μM ve 100 μM ISY konsantrasyonları ile 25, 50 ve 100 J/cm2 lazer kullanılan gruplar birbirleri ile kıyaslanmıştır. Yapılan çalışmalar sonucunda ISY yüklü AuNP'lerin toksik etki gösterdiği saptanmıştır. Aynı zamanda kolon kanseri hücrelerinin prostat kanserine kıyasla AuNP-ISY ile yapılan FDT'ye daha dirençli olduğu gözlemlenmiştir. PC-3 hücrelerinde toksik etki olmaksızın hücre canlılığında anlamlı bir düşüş olmamakla birlikte, PC-3 hücreleri kontrol grubuna göre anlamlı düşüş göstermiştir. Caco-2 hücrelerinde ise bu anlamlı düşüş daha yüksek dozajlarda ve yüksek enerji yoğunluğunda gözlemlenmiştir.

Anahtar Sözcükler: Fotodinamik Terapi, Prostat Kanseri, Kolon Kanseri, İndosiyanin Yeşili, Altın Nanoparçacıklar.

TABLE OF CONTENTS

LIST OF FIGURES

LIST OF TABLES

LIST OF SYMBOLS

F	Absorption correction factor
Au	Gold
J	Joule
OD	Optical density
m	Slope of a curve
ϕ	Singlet oxygen quantum yield
$^1O_2$	Singlet state oxygen
V	Volt
W	Watt

LIST OF ABBREVIATIONS

ALA	Aminolevulinic Acid
Caco-2	Human Colorectal Adenocarcinoma Cancer Cell Line
DLS	Dynamic Light Scattering
DPBF	1,3-diphenylisobenzofuran
ER	Endoplasmic Reticulum
HPD	Hematoporphyrin Derivative
ICG	Indocyanine Green
MB	Methylene Blue
MDR	Multi Drug Resistance
MNP	Metallic Nanoparticle
NIR	Near-infrared
NP	Nanoparticle
NR	Nanorod
PC-3	Human Prostate Adenocarcinoma Cell Line
PDT	Photodynamic Therapy
PEI	Polyethylenimine
PS	Photosensitizer
PTT	Photothermal Therapy
ROS	Reactive Oxygen Species
RT	Radiation Therapy
SEM	Scanning Electron Microscope
SPR	Surface Plasmon Resonance

1. INTRODUCTION

1.1 Motivation

Cancer is the world's second leading cause of death, making it a critical health issue. There have been serious disadvantages of conventional therapies [1]. Although, the traditional cancer treatment methods have been developed in recent years, including chemotherapy and radiation therapy, new treatment methods are widely researched due to their inefficacy especially in the chemical therapy of malignant tumors. Multidrug resistance (MDR) due to repeated drug administration is the major causes of therapy failure following chemical therapy and radiation therapy (RT) [1], [2]. Total resection of tumor lesions is often difficult because in many cases of cancer they are tangled with healthy tissues. Clinical oncology has started to move from monotherapy to combination treatment. The concept of synergistic treatment includes the combination of two or more treatment techniques in one platform, resulting in much greater results [1].

Photodynamic therapy is promising as a minimally invasive method among the studies on cancer treatment and new methods developed in recent years. PDT has proven its efficacy in various cancer types. Radiotherapy and chemotherapy were also effectively coupled with PDT [3]. Photodynamic therapy in cancer treatment; it is advantageous in that it does not damage healthy cells when targeting cancer cells and can be repeated without limitation, in contrast to conventional methods.

Among the molecules proposed to be used as photosensitizers in the literature, ICG is particularly notable for its absorption spectrum within the tissue optical window and it has negligible toxicity in the dark. There are some studies about the use of ICG for PDT applications in the literature. However, this physiological dye, which is highly stable in powder form, can rapidly degrade in aqueous solutions. They begin to form clusters and rapidly lose their photosensitizing properties by binding to proteins in the

presence of proteins [4]–[5]. This is one of the most important drawbacks of the ICG.

Nanoparticle-based drug carriers are used for many drugs in order to increase the solubility, stability, and effects of drugs. In order to overcome the disadvantages of ICG, the transportation of it with the help of nanoparticles is a promising approach. ICG was previously loaded into various polymeric carriers such as Poly Lactic-co-Glycolic Acid (PLGA), chitosan, and dextran, and photodynamic and photothermal studies were performed on various cell types. Although the number of studies performed with ICG on gold nanoparticles is few, it shows stronger photothermal effects thanks to the adjustable absorption spectra of gold nanoparticles [6]–[7]. Combining gold nanoparticles and ICG for a PDT treatment approach is a promising study that can overcome the drawbacks of the photosensitizer.

1.2 Outline of the Thesis

Chapter 1: The thesis is introduced and the motivation of the study is presented.

Chapter 2: The necessary background information about cancer in general, therapy-related challenges, the incidence of prostate and colon cancers is given. Photodynamic therapy and photosensitizers, as well as nanoparticles used in drug delivery are discussed. A literature review of the use of gold nanoparticles as indocyanine green carrier for PDT is provided.

Chapter 3: Aim of the study is proposed.

Chapter 4: Steps need to be followed to achieve the aim are listed.

Chapter 5: Information about the experimental materials and the methods used for the research is presented.

Chapter 6: Results and findings obtained in this study are given.

Chapter 7: Results of this study and their implications are discussed.

Chapter 8: Conclusion and possible further works of the proposed study are given.

2. BACKGROUND

2.1 Cancer

Uncontrolled proliferation of abnormal cells any different kinds of cells in the body is called cancer. Below is a scheme (Figure 2.1) which demonstrates the usual cell division and how the cell generally dies when it is damaged or transformed. It is also shown what happens when those cells do not die. They become cancer cells and uncontrolled division results in a mass of tumor cells.

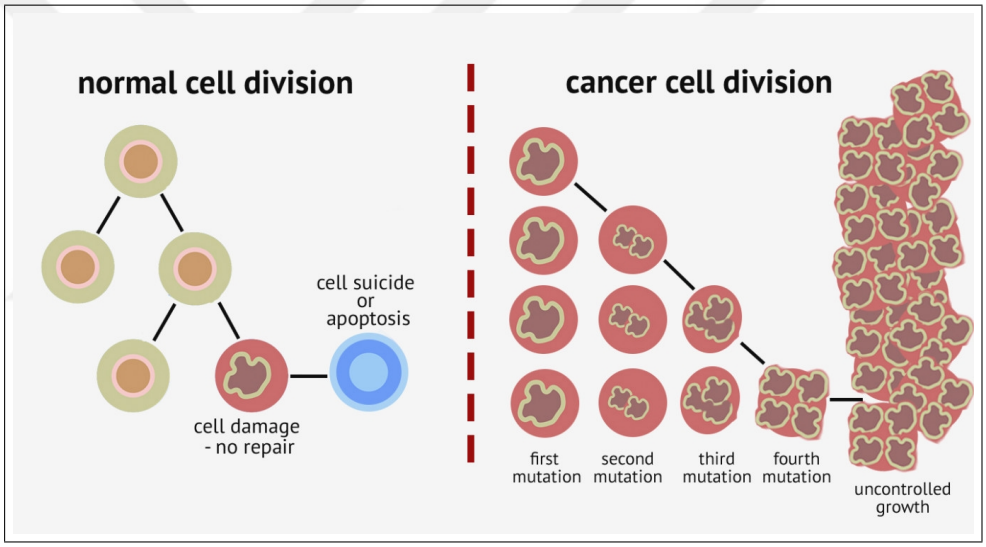

Figure 2.1 Abnormal cell division [8].

This proliferated cell mass is called tumor which could be benign or malignant. The distinction between benign and malignant tumors is the primary issue in cancer pathology. A benign tumor stays restricted to its initial place, not invading surrounding environment or spreading to other areas of the body (Figure 2.2). However, a malignant tumor can both invade the surrounding environment and spread through the circulatory or lymphatic systems which result in metastasis. Just malignant tumors accurately identified as cancers that make cancer so hazardous because of their capacity to invade and metastasize. While benign tumors can generally be removed by a surgeon, malignant tumors are often resistant to such surgery because of the spreading behavior.

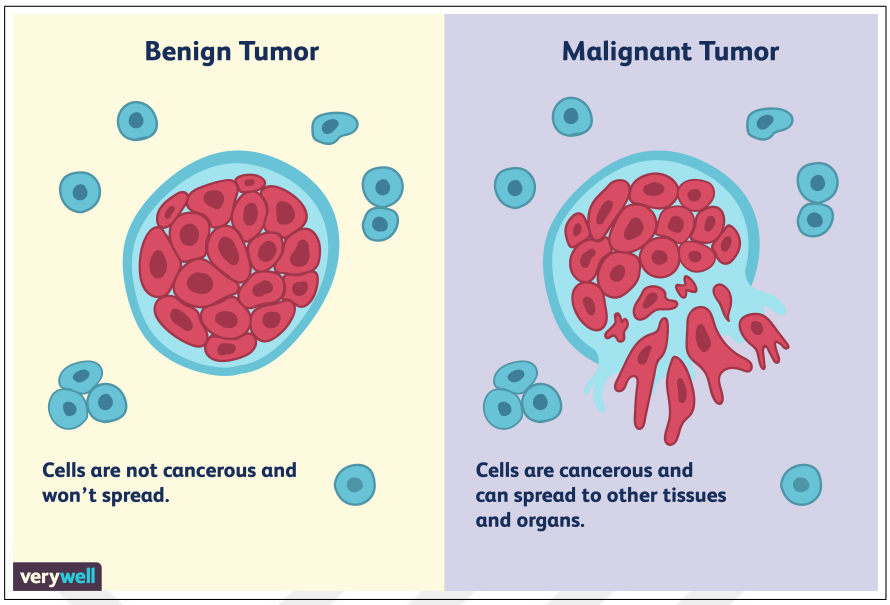

Figure 2.2 Difference between benign and malignant tumor[9].

The cell type that benign and malignant tumors originated from classifies it. Cancer tissue identified by the name of the tissue that the abnormal cells arose from such as colorectal cancer, lung cancer, breast cancer. Carcinoma, sarcoma, leukemia or lymphoma are the primary classes of cancers. The malignancies of epithelial cells are carcinomas that constitute 90% of human cancers. Sarcomas are solid connective tissue tumors, such as muscle, bone, cartilage, and fibrous tissue, which are not common in humans. Blood-forming cells and cells in the immune system generate leukemia or lymphomas, which account for roughly 8% of human malignancies.

Cancer-causing substances, known as carcinogenic agents, have been recognized by research in experimental animals as well as by epidemiological studies of cancer in human populations. Because malignancy is a complicated multi-step mechanism, many variables may influence the probability of cancer development. However, there have been many factors discovered in both animals and human experiment which lead to cancer, including radiation, chemical and viruses [10]. Although the causes of cancer are not fully understood, many factors that boost the disease incidence can be modifiable like smoking and excess body weight and others cannot such as heritable genetic mutations and immune conditions. The development of cancer could be triggered and/or supported simultaneously or sequentially by these risk elements [11].

Although many types of cancer happen, only a few appear often (Table 2.1). More than one million cancer cases in the United States are diagnosed annually, and over 500,000 people die from cancer every year.

Table 2.1
Ten Most Frequent Cancers in the United States [10].

Cancer site	**Cancer per year**	**Deaths per year**
Breast	184,200 (15.1%)	41,200 (7.5%)
Prostate	180,400 (14.8%)	31,900 (5.8%)
Lung	164,100 (13.4%)	156,900 (28.4%)
Colon/rectum	130,200 (10.7%)	56,300 (10.2%)
Lymphomas	62,300 (5.1%)	27,500 (5.0%)
Bladder	53,200 (4.4%)	12,200 (2.2%)
Uterus	48,900 (4.0%)	11,100 (2.0%)
Skin (melanoma)	47,700 (3.9%)	7,700 (1.4%)
Kidney	31,200 (2.6%)	11,900 (2.2%)
Leukemias	30,800 (2.5%)	12,100 (2.2%)
Subtotal	933,000 (76.5%)	368,800 (66.8%)
All sites	1,220,100 (100%)	552,200 (100%)

More than 75% of this total cancer incidence is due to cancers at 10 distinct body locations. The four most frequently reported cancer instances which create more than half of all cancers are breast, prostate, lung and colon/rectum [10]. 2019 estimations of American Cancer Society about leading sites of new cancer cases and deaths shown below (Figure 2.3).

Prostate cancer has the highest occurance rate in males and colon cancer has a high rate in both male and female [11]. A benign polyp initiates colon cancer and develops into a higher degree dysplasia adenoma and then becomes an invasive cancer. Two types (hyperplastic and adenomatous) are primarily malignant polyps. Due to the uncontrolled growth of glandular cells holding small quantities of cytoplasm, the development of hyperplastic polyps is triggered.

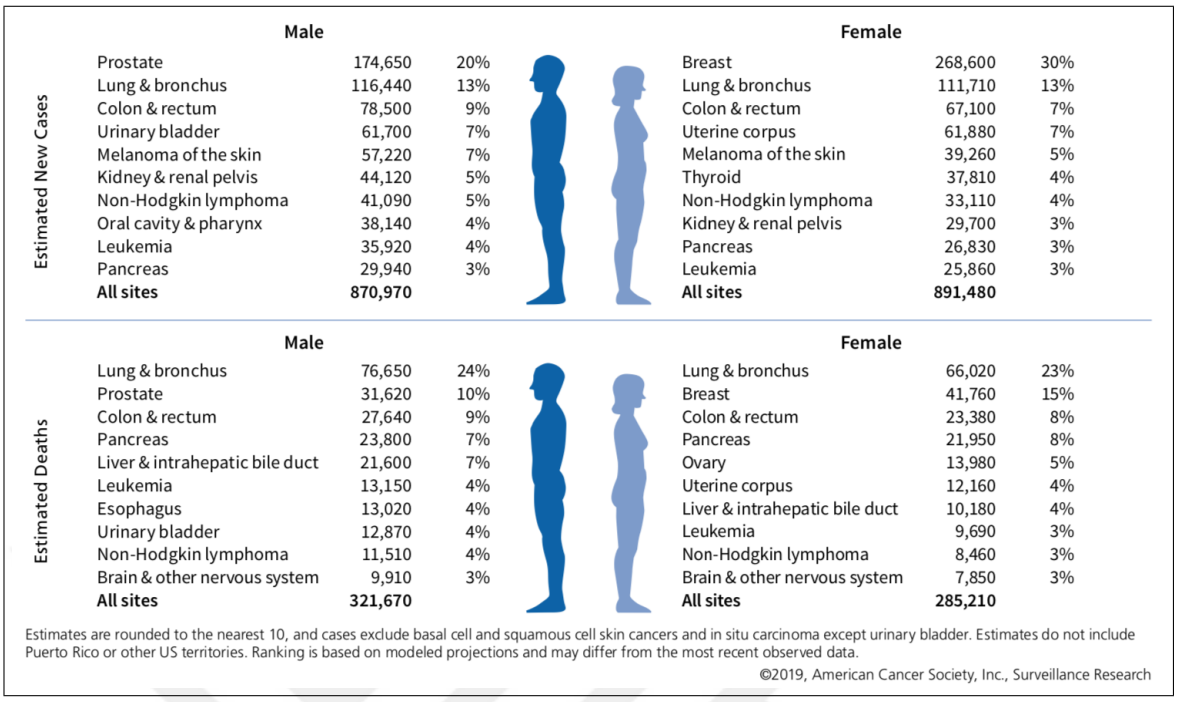

Estimated New Cases

Male			Female		
Prostate	174,650	20%	Breast	268,600	30%
Lung & bronchus	116,440	13%	Lung & bronchus	111,710	13%
Colon & rectum	78,500	9%	Colon & rectum	67,100	7%
Urinary bladder	61,700	7%	Uterine corpus	61,880	7%
Melanoma of the skin	57,220	7%	Melanoma of the skin	39,260	5%
Kidney & renal pelvis	44,120	5%	Thyroid	37,810	4%
Non-Hodgkin lymphoma	41,090	5%	Non-Hodgkin lymphoma	33,110	4%
Oral cavity & pharynx	38,140	4%	Kidney & renal pelvis	29,700	3%
Leukemia	35,920	4%	Pancreas	26,830	3%
Pancreas	29,940	3%	Leukemia	25,860	3%
All sites	**870,970**		**All sites**	**891,480**	

Estimated Deaths

Male			Female		
Lung & bronchus	76,650	24%	Lung & bronchus	66,020	23%
Prostate	31,620	10%	Breast	41,760	15%
Colon & rectum	27,640	9%	Colon & rectum	23,380	8%
Pancreas	23,800	7%	Pancreas	21,950	8%
Liver & intrahepatic bile duct	21,600	7%	Ovary	13,980	5%
Leukemia	13,150	4%	Uterine corpus	12,160	4%
Esophagus	13,020	4%	Liver & intrahepatic bile duct	10,180	4%
Urinary bladder	12,870	4%	Leukemia	9,690	3%
Non-Hodgkin lymphoma	11,510	4%	Non-Hodgkin lymphoma	8,460	3%
Brain & other nervous system	9,910	3%	Brain & other nervous system	7,850	3%
All sites	**321,670**		**All sites**	**285,210**	

Estimates are rounded to the nearest 10, and cases exclude basal cell and squamous cell skin cancers and in situ carcinoma except urinary bladder. Estimates do not include Puerto Rico or other US territories. Ranking is based on modeled projections and may differ from the most recent observed data.

Figure 2.3 Leading sites of new cancer cases and deaths [11].

The third most popular type of cancer that causes disease and the fourth widespread type of cancer that causes death in the world is colon cancer. It is the only form of cancer that has the same occurance frequency in both genders. Colon cancer is generally seen in the population with a poor lifestyle, obesity, drinking, and smoking. Previously, those instances were mostly found in individuals over 50–60 years of age but recent cases have seen in younger patients [12]. In the United States, approximately 101,420 colon and 44,180 rectal cancer cases will be diagnosed in 2019. The incidence of colorectal cancer has decreased over several decades as risk factor exposures and screening has changed. On the other hand, the general pattern driven by older adults and it bring about overlook of the increase in younger age group incidences. The incidence levels of adolescents 55 years of age and older decreased by 3.7 percent per year from 2006 to 2015 but increased annually by 1.8 percent among those under the age of 55 [11].

In 2019, 51.020 colorectal cancer deaths are estimated. Unfortunately, precise statistics are not accessible on separate colon and rectal cancer fatalities due to misclassification of rectal cancer on the death certificate as colon cancer. The extensive use of

the word "colon cancer" to involve both colon and rectal cancers in education messages mainly causing this classification. The death rate at 55 and older people dropped by 2.7% each year, while adults under 55 years of age increased by 1% every year during 2007-2016. Colorectal cancer has a survival rate of 65% for 5 years. Localized diseases (39% of patients) 5 year survival is 90% [11].

Rectal bleeding, blood in the stool, changes in bowel patterns or stool shape, feeling that the bowel is not entirely empty, abdominal discomfort, reduced appetite, and weight loss are some of the symptoms. Cancer promoted blood loss in some people causes anemia, which results in weakness and exhaustion. Colorectal cancer in the early stage generally has no signs, so screening is required to early diagnose.

Surgery, standard chemotherapy, radiation therapy, and directed molecules are all four main therapies for colon cancer [13]. Colorectal cancer surgery is the most prevalent therapy for not spreading types. Apermanent colostomy is rarely essential for colon cancer. Metastatic colorectal cancer treatment typically requires chemotherapy and/or targeted therapy. In some advanced cases, immunotherapy is a newer alternative [11]. Overall, treatment choice affected by the phase of cancer. At early cancer stage (0 to 1 stage), laparoscopy, colostomy or radiofrequency ablation (RFA) surgeries are common methods. Chemotherapy may also be evaluated for critical patients with stage 2 cancer according to the cruciality of the cancer. In the third phase, chemotherapy is also recommended for faster rehabilitation after getting surgery. Chemotherapy by standard or directed molecules is crucial in case of metastasis meaning stage 4 cancer [13].

The therapy methods available to fight colon cancer are obviously inadequate. The main weaknesses are impacts on healthy cells of chemotherapy agents, a large cost of targeted chemotherapy, cancer recurrence and drug resistance [13].

Prostate cancer incidence fell by approximately 7 percent per year from 2011 to 2015. In the United States, approximately 174 650 current prostate cancer instances were reported during 2019. The occurrence in blacks is approximately 60% greater

than in whites [11]. The number of males having prostate cancer has fallen by 2.4 percent per year between 2000 and 2006. About one in 6 male has prostate cancer and one out of every 36 will die because of it [14].

Prostate cancer risk factors are African ancestry, older age (Men older than 65 years of age generate 75% of the prostate cancer cases and also it is uncommon to see it younger than age 40), a relative having the disease (the risk is two-fold if the patient has a first degree relative with the cancer), and some genetic factors which can be inherited like Lynch syndrome and BRCA1 and BRCA2 mutations.

Prostate cancers in the early stages are generally asymptomatic. The advanced disease has similar signs with benign prostate terms, such as low or disrupted urinary stream, frequent urinating need, nocturia, urinary blood, pain or burning with urination, hesitancy, incomplete emptying, and various degrees of incontinence. Hip, backbone, rib, or other pain could be seen in late-stage cancer due to spreading to bones[11][14]. Most of the prostate cancers (90%) diagnosed at a local or regional stage. At these stages, the survival rate of five years is nearly 100%. At distant stages, the rate becomes 30% and at all stages, it becomes 98% for ten-year survival [11].

Adenocarcinoma causes for more than 95% of prostate cancer. It develops from epithelial cells of prostate gland. A histological assessment of prostate tissue biopsy extracted from a prostate needle covers the diagnosis of prostate cancer. Treatment decisions based on the staging of cancer. The age of the patient, the severity of the disease, and conflicting comorbidities should be considered by the clinician when deciding therapy methods. Therapy options can be investigated in two main groups; options for localized prostate cancer and advanced prostate cancer. For localized diseases, active surveillance, radical prostatectomy, brachytherapy (radioactive seed implants), cryotherapy and, External Beam Radiation Therapy (XRT) are common treatment options. Hormone treatment, chemotherapy, radiation treatment are used to treat prostate cancer which is spreading to distant locations. Recurrent prostate cancer following treatment, recurring local cancer or systemic and clinical recurrence denote advanced prostate cancer. Advanced prostate cancer can be managed with hormone

therapy by reducing its size or restricting its development, thereby assisting to ease pain and other symptoms. Together with hormone treatment, chemotherapy may be performed or used alone when hormone treatment is no longer efficient. A cancer vaccine to boost the immune system of the patient to attack prostatic cancer cells precisely is an alternative for developed prostate cancer which no longer reacts to hormones[11][14]. Unfortunately, prostate cancer therapies have some adverse effects shown in Table 2.2 [14].

Cancer is the second major cause of death in the world, that makes it a crucial health problem. Serious drawbacks have been faced with conventional therapies, so generally, they are not enough to get successful results [1]. Although there are many works being made to get pleasing results from cancer treatments, they did not give excellent outcomes. Traditional cancer treatment methods including surgery, chemotherapy and RT have advanced in the last few years. However, there is a common failure in chemical therapy for malignant tumors by cytotoxic drugs. The main cause of therapy failure following chemotherapy and RT, is MDR because of repeated administration of drugs. Many kinds of tumors are often resistant to most cytotoxic drugs from the beginning. Other tumors may react at the beginning, but subsequently, also seem resistant [1][2].

In conclusion, conventional cancer therapy solutions have significant disadvantages which are not often satisfying when used in a single modality. Complete tumor lesions resection is often problematic because they are tangled with healthy tissues in many instances of cancer. The impact of certain therapies usually shows increased effectiveness, in combination with other modalities. In recent years, clinical oncology has a tendency to shift from monotherapy to combination therapy. The principle of synergistic therapy involves combining two or more methods of treatment in one platform, which results in far greater therapeutic effects than using the respective monotherapies separately. The rational combination of different therapy types with the understanding of the underlying mechanisms involved in each combination would help to achieve a win-win approach by gathering benefits and compensating the drawbacks of each therapy [1]. In modern oncology, merging different treatment approaches while their toxicities are not overlapping is one of the most widely used solutions for developing a

therapeutic index.

Photodynamic Therapy has proven its efficacy in superficial cancer of the bladder, Barrett's esophagus, early and obstructive lung cancer, skin, head and neck cancers. It is also used to decrease the remaining tumor mass by using as a supportive therapy after or during surgery [15]. The antitumor efficacy of PDT can be improved by two main methods; sensitizing tumor cells with PDT and interference with cytoprotective molecular responses caused by PDT in tumor or stromal cells that survive. PDT uses photosensitizer (PS) as an activating agent. PS interactions will be restricted with the illumination area. Thus, the toxicity of the components is not systemic. Older and incapacitated patients who cannot tolerate more comprehensive therapy can benefit from this specialty of PDT. Furthermore, PDT may be coupled with other anti-tumor therapies securely without the danger of causing cross-resistance in view of its special $^1O_2$ dependent cytotoxic impacts. Only several trials have been conducted about PDT combinations with conventional anti-tumor treatments. PDT can be used as presurgery, adjuvant or repetitive treatment. Radiotherapy and chemotherapy were also effectively coupled with PDT [3].

The enhanced PS delivery is another strategy for improving PDT efficacy. Conjugating PSs with different tumor-targeting molecules is a good approach in order to achieve that purpose. That is essential for the therapy of tumors where wide regions of the surface are exposed therapy, thus an increase in tumor selectivity is required in such cases like superficial bladder growing cancer or pleural and peritoneal cavity metastases. Targeted antitumor drugs enhanced the range of combinations that influence tumor cells with miscellaneous molecular mechanisms by cytotoxicity of PDT. Proteins represent almost 70% of dry cell weight, so they are the main targets for oxidative reactions. Molecular chaperones such as heat shock proteins can refold oxidized proteins. On this occasion, misfolded proteins accumulate and aggregate. A mechanism called endoplasmic reticulum (ER) stress can be provoked by the accumulation of misfolded proteins within ER which can result in cell death. In order to expose tumor cells to PDT, interfering with refolding or removal of oxidized proteins can be adopted as a therapeutic approach. In order to effectively treat hematologic disorders, bortezomib, a

proteasome inhibitor, potentiates the cytotoxic impacts of ER stress which leads to an increase in the cytotoxic effect of PDT. Deeply localized cells within the tumor mass acquire suboptimal light doses and survive by courtesy of various cytoprotective processes. Selective inhibitors have demonstrated improved antitumor efficiency of PDT by targeting enzymes involved in reactive oxygen species (ROS) production. Cyclooxygenase (COX) inhibitors, anti-angiogenetic or anti-vascular medicines, monoclonal antibodies targeting neovascularization factors can trigger additional anti-vascular properties of PDT. The tumor growth management after PDT can be considerably improved. Moreover, it can be possible to enhance the efficiency of PDT by combining with agents that target signal transduction pathways. The combination of two PSs in a single therapy also results in tumor and vascular cells simultaneously targeted.

A research released on the impacts of hematoporphyrin derivative (HPD) illuminated with light in 5 bladder cancer patients at the end of the 1970s [16]. The first wide range of patients effectively handled with PDT using HPD as photosensitizer was revealed by Dougherty et al in 1978. In 111 of 113 malignant lesions, the complete or partial reaction was noted. None were discovered to be irresponsive of the wide range of tumors investigated [17]. More than 200 clinical trials for PDT have taken place since then. Systemic reviews have recently shown that in the therapy of malignant and premalignant nonmelanoma skin lesions PDT could be a feasible choice. Despite Barrett esophagus and unresectable cholangiocarcinoma could also benefit from PDT, it has not yet clearly demonstrated that PDT is efficient in the treatment of other cancers. This is mainly because there are only a few randomized controlled studies have been carried out. A systematic literature assessment is constrained because the studies do not have optimal PDT parameters (PS dose, illumination conditions) that can be compared with each other. The impacts of PDT are mainly superficial. The range of tumor destruction varies from a few millimeters to 1 centimeter because of the restricted light penetration through the tissue. This seeming benefit can be used positively in the therapy of peripheral illnesses, such as premalignant circumstances, (mucous dysplasia, actinous keratosis), in situ carcinoma, and peripheral tumors such as intraperitoneal, pleural mesothelioma can take advantage of this limitation of PDT. In addition, PDT may support the operation by irradiating the environment of tumors

and boost the likelihood of local disease control in the long-term.

There are limited choices for recovery of isolated local failure for patients with prostate cancer who choose to undergo definitive radiotherapy. In addition, treatment for early prostate cancer is correlated with important morbidities owing to its closeness to organs such as bladder and rectum. Visible light damage caused by PDT has the capacity to treat prostate cancer selectively and save the surrounding tissues. The light can be transmitted to the prostate glands through interstitial, cylindrical diffusing optic fibers by adjusting the methods created for brachytherapy. The mechanism of cell death caused by PDT does not similar to chemotherapy or RT which kills cells by damaging their DNA or affecting cell cycle, so cross-resistance and late normal tissue occurrences such as secondary cancer possibility decrease. Owing to all these challenges, prostate cancer becomes an appealing issue to experiment on. All of the trials show the need for extensive treating of the whole prostate gland, even if PDT for the prostate is feasible. Enhanced methods and dosimetry are very important for an appropriate toxicity profile.

2.2 Photodynamic Therapy and Photosensitizers

Photodynamic Therapy is a treatment method that is minimally invasive and selective for cancer treatment and bacterial infection [15][18]. Photosensitizer, light, and oxygen are the three main components of PDT. Each of them is nontoxic, however, they trigger a photochemical reaction that results in the production of singlet oxygen. It includes the administration of a photosensitizer that is tumor-localized and then local illumination of the tumor with a specific wavelength to trigger PS. PDT procedure can be carried out by the systemic, local or topical administration of a PS which is a nontoxic drug or dye, later on, the photosensitized area is illuminated with a visible light source after a certain amount of time. The excited PS gives energy to molecular oxygen and generates ROS which can lead to cell death and tissue destruction by apoptosis or necrosis [15][3][19].

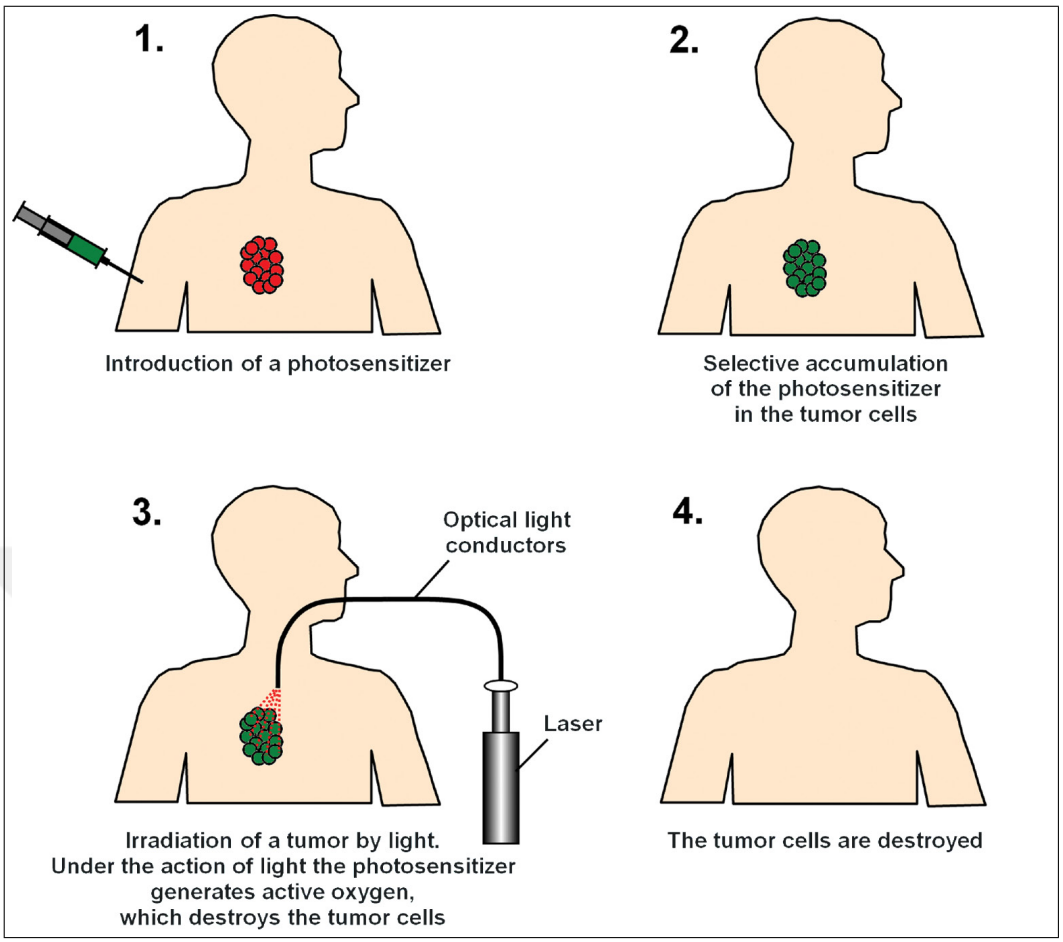

Figure 2.4 Demonstration of an anti-tumor PDT application [20].

Therapy mechanisms are significantly influenced by the type and dose of the PS. Moreover, the period of the time between the administration of the PS and light exposure should be chosen delicately. Total light dose and fluence rate also have a quite effect on PDT results. Consequently, collaborative work is needed to determine the ideal circumstances for PDT [3].

Two types of responses can occur when the PS excited to triplet state (Figure 2.5). Type I response allows the cell membrane or molecule to react directly to the PS and transferring a proton or an electron into a radical anion or cation. These radicals can produce reactive oxygen species by interacting with oxygen. On the other hand, in a type II reaction, on the purpose of creating excited-state singlet oxygen, the triplet PS can transform its energy to molecular oxygen. The responses of Type I and Type II reactions can happen at the same time and their frequency depends on the sort of PS,

substrate and oxygen levels presenting. Nevertheless, many researches express Type II responses, thus $^1O_2$ has the major importance to achieve PDT [15][19][21].

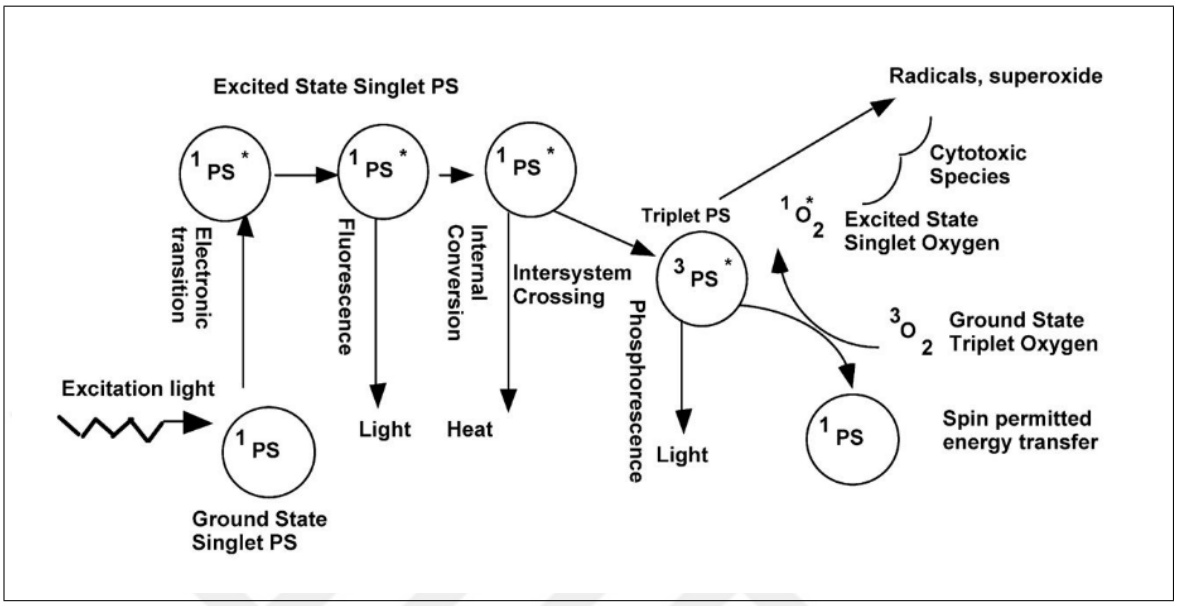

Figure 2.5 Photophysical and photochemical mechanisms of PDT [19].

The amount of tumor destruction after PDT depends on the type of PS, the concentration and location of it, its subcellular position at the time of irradiation, drug administration and light exposure interval, light fluency rates, total exposure, tumor type, oxygenation level. Tumor cells, microvasculature, immune and inflammatory systems are PDT targets to achieve tumor destruction. ROS is the main component that causes tumor and microvascular deformation in an irreversible manner. Whereas vascular damage and direct killing of the tumor cells are the primary reason for the initial ablation of the tumor, antitumor immune response and immune system improvement could have a significant function in secondary cytotoxicity, helping to enhance tumor response to the PDT [15][21].

An ideal photosensitizer should be a pure compound with a low cost of production and have a decent shelf-life. The absorption peak should within the range of 600 and 800 nanometers. First of all, absorption bands at shorter wavelengths have less tissue penetration because endogenous molecules like hemoglobin have strong light absorption below 700 nm. Furthermore, low-wavelength treatment requires a higher dose

of PS and may lead to photosensitivity of the skin. Secondly, the absorption of photons longer than 800 nm provides insufficient energy to excite oxygen to singlet oxygen which is needed for ROS production. Whereas red or infrared radiation propagates deeply, blue light penetrates less effectively through tissue. Since light penetration increases with wavelength, tumor control can be improved with strong absorbance at higher wavelengths especially in the deep red (Figure 2.6) [3][19]. Some other characteristic that a PS should show is amphilicity for a successful systemic travel to the tumor. While hydrophilicity is required for successful travel in the body, lipophilicity is required due to bonding to the target cells [15]. It should have low dark toxicity and rapid clearance from healthy tissue while accumulating selectively in tumor tissue to reduce phototoxic side effects. Even if there is generally a long waiting time before light irradiation, to give time for PS clearance from healthy tissue, there are recent studies indicate that the tumor response may improves when light irradiation comes after a shorter interval with the intention of leaving PS remains in the blood vessels to cause vascular damage. In addition, a short period between injection and irradiation is beneficial to enable patient-friendly and cost-effective outpatient treatment. Due to the absence of anesthesia or intense sedation during PDT, pain on therapy is unwanted. At last, photobleaching meaning destruction of the PS during illumination has been considered unwanted. However, several studies claim that light dosimetry can be less vital as overtreatment is avoided when photobleaching occurred [3][19].

Water-soluble HPD, a purified form of porfimer sodium subsequently recognized as Photofrin is the first PS clinically used in cancer therapy. Porfimer sodium has many advances like efficiently destroying tumors, negligible dark toxicity, and can readily be produced in a water-soluble preparation to deliver intravenously. While porfimer sodium remains the most frequently used PS, it has certain disadvantages, such as long-lasting photosensitivity and comparatively low absorption at 630 nm. Its efficiency can be enhanced by shifting the range of absorption at longer wavelengths.

A significant attempt has done to discover second generation PSs, several hundred potential substances suggested to be useful for PDT anti-cancer treatments. The maximum absorption of these PSs is generally over 630 nm and they have higher ex-

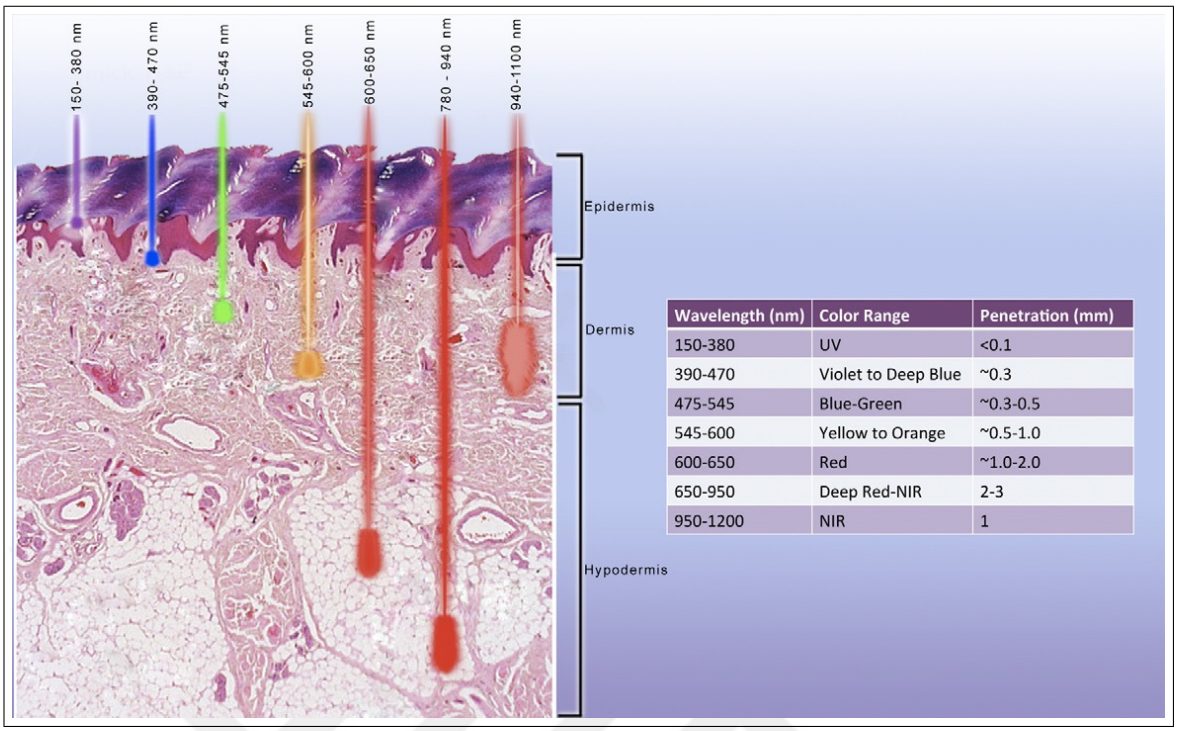

Figure 2.6 Light Penetration Depths in Tissue [22].

tinction coefficients. Higher quantum yields were presented by the second-generation PS, also accumulation in the tumor cell properties better than HPD. In addition, PDT can be carried out at the day that the drug is administered thanks to faster accumulation in tumor cells and clearance from normal cells. Thus, PDT can be performed out-patient. While some second-generation photosensitizers including aminolevulinic acid (ALA) are hydrophilic, generally they are extremely hydrophobic. The extent of PS hydrophobicity is known to influence its administration and biodistribution. While PS can enter through the cell membrane and find its way to the photosensitive subcellular environment, extremely hydrophobic PS can aggregate in an aqueous solution including physiological solvents and body fluids, so its clinical use will be restricted. Thereby, clinically efficient PS's hydrophilicity and lipophilicity must be balanced.

Developing 3rd generation PSs encloses most of the research going on now. Desired characteristics are an absorption peak at a longer wavelength, shorter photosensitivity after treatment and, above all, better selectivity of the tumor. Either by altering current PSs using biological conjugates, including peptides, an antibody for a

tumor-specific targeting or encapsulation of PS in order to easier travel in the blood from the place of administration to the target [15].

Indocyanine green is an anionic dye that is widely applied in clinical diagnosis for cardiac output, blood volume, liver function, pharmacokinetic analysis [24][4]. It has low toxicity at dark and hydrophilic characteristic. ICG can produce ROS when activated with near-infrared (NIR) light [25]. Activation by NIR light makes it preferable due to deeper tissue penetration. Its absorption peak changes slightly depending upon concentration, but it generally has an absorption peak at 800 nm which is longer than many other PS [4].

2.3 Nanoparticles

Nanoparticles are submicroscopic particles with dimensions of 1 to 100 nm that can fulfill most of the needs of traditional PS used in PDT. Nanoparticles are made from a range of natural or synthetic materials [26]. Biodegradable polymers, ceramic (silica), metallic (gold, silver) NPs; magnetic NPs, upconverting NPs are some of the approaches [3].

NPs are promising carriers thanks to their several benefits, including reducing drug toxicity and controlled drug release, conducting theragnostic tasks through providing multimodal imaging while enabling diagnosis and therapy. Their functionalization properties also make them practical for various intended purposes by modifying their surfaces with different components such as functional and chemical groups, biological molecules and radioactive agents (Figure 2.7). They have high surface/volume ratios and thereby the PS can be transferred to the target cells will be boosted. The early release of PS and possible inactivation of it could be reduced by the use of nanoparticles. Accordingly, better target specific accumulation and altered photosensitivity achieved. Their ability to deliver hydrophobic and/or hydrophilic drug molecules improves transportation features in the bloodstream, thus have better tumor localization. They also have the advantage of imprcoved permeability across biological barriers and

compartments [15][26][27].

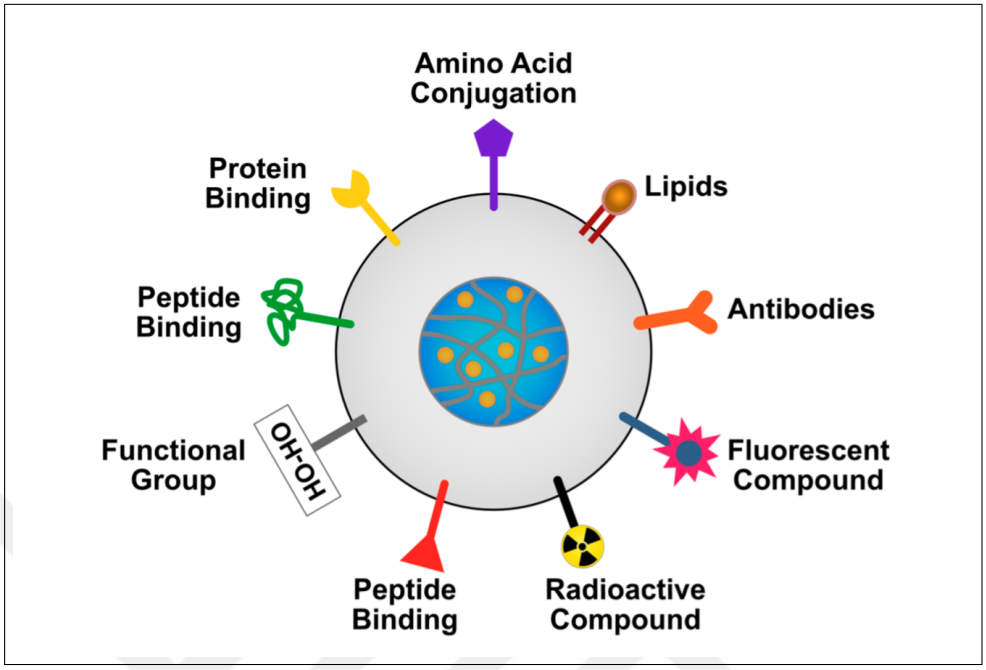

Figure 2.7 Various methods of modifying nanoparticle (NP) surfaces to target cancer cells [27].

Non-biodegradable nanoparticles are not favored as drug carriers due to their inability to decompose or controlled release of drugs. Nevertheless, in PDT as a multifunctional theragnostic carrier, nonbiodegradable nanoparticles have aroused interest with their outstanding features, including its optical properties and tunability of their size and shape easily [15].

2.3.1 Gold Nanoparticles

In the biomedical sciences and engineering, metallic nanoparticle (MNP) has been used extensively. MNPs can be produced and altered with several chemical functional groups to be used for distinct biomedical applications. They can be produced in different shapes like nanowires, nanorods, sheets and pads, nanoshells, nanocages, etc. The optical properties of MNPs are distinctive in shape and size. Therefore, their shape can be tuned for the desired purpose. Silver, gold, palladium, platinum, iron oxide, zinc oxide are some of the MNPs that has been used commonly. Furthermore, in comparison with other nanoparticles, such as micelle-driven particles, the inorganic

nanocarrier's structure is more stable.

AuNPs are widely used as effective drug delivery products for tumor targeting because of their non-toxic and non-immunogenic properties [27]. A combination of distinctive characteristics such as the surface plasmon resonance (SPR) and transforming light energy to thermal energy make photothermal therapy (PTT) possible. SPR improve the excitation efficiency of the accompanying PS. The innovation of a multipurpose AuNP that offers synergistic therapeutic application such as PTT and PDT has been a new trend in the field [15].

2.3.1.1 Gold nanoparticles conjugated with ICG. The distinctive aspect of surface plasmon resonance, enhancing the absorption in NIR band, ensures gold nanoparticles to being feasible compounds in cancer theranostics. On the other hand, ICG is an outstanding NIR imaging agent, as well as an ideal light absorber for PDT and PTT [28]. Au nanorods (NRs) and Au nanoparticles (NPs) are convenient approaches to enhance the photostability of ICG. The previous research indicates that photo-destruction with simultaneous PTT and PDT can be achieved by ICG implemented gold NRs [29]. They are also extremely chemically stable non-linear optical bio-imaging materials in the NIR region. The combined PTT and PDT processes are more efficient with respect to their singular effects for each Au NRs and Au NPs based ICG photosensitizer. For the Au-ICG NPs studies shows improved efficacy depending on the size of NP [30].

In addition to the synergistic effect of PDT-PTT, improved permeability and retention impact of the synthetic gold nanoclusters-indocyanine green nanoprobes produced by Cui et al. proved an improved cellular absorption and efficient tumor targeting [31]. Li et al. demonstrated that covalent conjugation of ICG and TNYL peptide (TNYL-ICG-HAuNS), with NIR light irradiation, had considerably improved light stability, ROS production, and photothermal effect. Their results show a great antitumor efficacy improvement. There is another study reporting the synergetic effect of PDT and PTT driven by the same group. Their nanoparticle manufactured using follow gold nanospheres (HAuNS) with the conjugation of ICG by branched polyethylenimine

(PEI, MW = 10 kDa), which ensured elevated ICG capacity. Meanwhile, provides a coating layer with appropriate density to keep ICG fluoresce and ROS production at efficient levels. As a result, the stability of ICG and selective tumor accumulation were remarkably increased compared to the free ICG. Compared with HAuNS alone, the ICG combination induced considerably greater plasmon absorption in the NIR, leading to an incredibly improved photothermal effect and also photodynamic impact [32]. In a different study conducted by Liu et al., both fluorescence and fluorodeoxyglucose positron emission tomography (FDG-PET) were used to collect the feedback from subcutaneous MDA-MB-231 mouse xenograft tumor model while AuNR-ICG mediated PDT applied. AuNR-ICG mediated PDT caused a significant decrease in the intensity of fluorescence and metabolic activity of tumors [33]. Luo et al. doped indocyanine green derivative (ICG-Der-02) into mesoporous silica-coated gold nanorods (AuNRs / mSiO2) then covered by a second layer of silica and combined with the α(v) integrin-targeting cyclic peptide (RGD-4C). Results of the study showed that human fibrosarcoma cells were preferably attached to their nanoconjugate and also dual modality PDT and PTT can be carried out at 808 nm irradiation [34]. In the research of Fang et al., ICG conjugated silica-coated gold nanorods (GNR@SiO2-ICG) synthesized. In vitro trials have shown that A375 cells died after laser irradiation thanks to the synergistic phototherapy effects of GNRs and ICG besides the GNR@SiO2-ICG showed great imaging properties [28].

Kuo et al. synthesized gold NPs and functionalized it in order to improve dual modality PDT and PTT. In mixing those NPs with the positive-charged PEI adsorbed on the surface of the Au NPs via electrostatic interaction, thus the surface of the Au NPs was transformed into a positively charged surface. Au-PEI NPs were merged with negatively charged ICG via electrostatic interaction. They also measure the temperature rise caused by an 808-nm (20 W / cm2) diode laser. Au-PEI-ICG NPs were superior photothermal agents than the ICG alone due to their findings. The anti-EGFR antibody has been conjugated with Au-PEI-ICG NPs for targeting. Targeting antibody dramatically affect the cell viability results. The viability of human lung carcinoma malignant cells (A549) was cells treated by ICG, 13 nm, 50 nm, and 100 nm Au-PEI-ICG are about 83%, 34%, 20%, and 8%, respectively. These findings

show that the efficacy of PDT and PTT improves with Au-PEI-ICG NPs compared to ICG only and the capacity to photochemically destruct cancer cells increases gradually depending on the size of Au NPs [30].

Table 2.2
Common Treatment Options of Prostate Cancer and Possible Side Effects of Treatments [14].

Treatment Option	**Disease Progression**	**Potential Adverse Effects**
Active surveillance	Localized	Illness uncertainty
External beam radiation	Localized and advanced disease	Urinary urgency and frequency, dysuria, diarrhea, and proctitis Erectile dysfunction Urinaryincontinence
Brachytherapy	Localized	Urinary urgency and frequency, dysuria, diarrhea, and proctitis Erectile dysfunction Urinary incontinence
Cryotherapy	Localized	Erectile dysfunction Urinary incontinence and retention Rectal pain and fistula
Hormone therapy	Advanced	Fatigue Hot flashes and flare effect Hyperlipidemia Insulin resistance Cardiovascular disease Anemia Osteoporosis Erectile dysfunction Cognitive deficits
Chemotherapy	Advanced	Myelosuppression Hypersensitivity reaction Gastrointestinal upset Peripheral

Table 2.3
A list of clinically applied photosensitizers [3] [15] [23].

Photosensitizier	**Typical Absorption Peak**
Porfimer Sodium (HpD) (Photofrin)	630 nm
ALA (Metvix, Levulan, Ameluz)	635 nm
Temoporfin (mTHPC) (Foscan)	652 nm
Tin etiopurpurin (Pyrlytin)	660 nm
Talaporfin	660 nm
HPPH	665 nm
Silicon phthalocyanines	670 nm
Sulfonated aluminium phthalocyanines (Photosens)	675 nm
Zinc phthalocyanines	675 nm
Verteporfin (BPD) (Verteporfin, Visudyne)	690 nm
Phthalocyanine	720 nm
Lutetium texaphyrin (Lutrin)	732 nm
Padoporfin (Tookad)	762 nm
Indocyanine Green (ICG) (Cardiogreen)	800 nm

3. AIM

NIR window applications ensure low scattering and energy absorption and maximum light penetration into the tissue. ICG strongly absorbs light in NIR region but there are certain constraints that restrict ICG as a photodynamic agent. One of the main constraints is its instability in aqueous solutions. The advantages of nanoscale drug carriers such as localized and targeted drug delivery, improved drug solubility and improved circulation time are known. Therefore, one of the methods that can be used to reduce the aggregation of ICG molecules and their binding to proteins is to load ICG into NP carriers to increase the effectiveness of ICG-PDT. The aim of the present study is investigating the efficiency of PDT on cancer cells using an 809-nm laser which has higher optical penetration in biological tissues compared to other lasers and AuNPs conjugated with ICG.

4. OBJECTIVES

The objectives of this study are

I. To accomplish the conjugation of ICG molecules with AuNPs by electrostatic interaction using PEI binding molecule.

II. To characterize the obtained particles by taking zeta potential and size measurements.

III. To investigate the changes in PDT effectiveness on Caco-2 and PC-3 cancer cell lines using ICG loaded Au NPs

IV. To compare the PDT efficacy of Au-ICG NPs with ICG alone.

V. To analyze the response of different cell lines to the therapies.

5. MATERIALS and METHODS

5.1 Cell Culture

Two different cancer cells to be used in this study (Caco-2 ATCC® HTB-37 ™ and PC-3 ATCC® CRL-1435 ™) were cultured in Bogazici University Biomedical Engineering Institute, Cell Culture Laboratory under routine culture conditions.

5.2 Experimental Groups

Groups of 25, 50 and 100 J/cm^2 laser were used as starting points on Caco-2 and PC-3 cell lines with ICG concentrations of 25 μM, 50 μM, 100 μM.

For selected ICG doses and power densities shown in Table 5.1, separately for both cell lines following experimental groups were formed.

- Negative Control (without ICG and Laser)
- Positive Control ICG (ICG only, in the dark)
- Au-ICG NP group (in the dark by applying Au-ICG NP only)
- PDT1 group (ICG and 809 nm laser)
- PDT2 group (Au-ICG NP and 809 nm laser)

Table 5.1
Experimental Groups

Caco-2	**PC-3**
	25 μM 25 J/cm^2
50 μM 25 J/cm^2	50 μM 25 J/cm^2
100 μM 25 J/cm^2	
	25 μM 50 J/cm^2
50 μM 50 J/cm^2	50 μM 50 J/cm^2
100 μM 50 J/cm^2	
	25 μM 100 J/cm^2
50 μM 100 J/cm^2	50 μM 100 J/cm^2
100 μM 100 J/cm^2	

5.3 Laser System

In this study, a diode laser with a wavelength of 809-nm was used. The laser used in the study is a computer-controlled and has 809 nm continuous mode radiation and a maximum power of 2000 mW.

In order to homogeneously illuminate more than one well at the same time, beam expander and collimator connected to the optical fiber end. The laser power density is fixed at 250 mW/cm^2 and the energy intensity is adjusted by controlling the irradiation time with the help of a shutter.

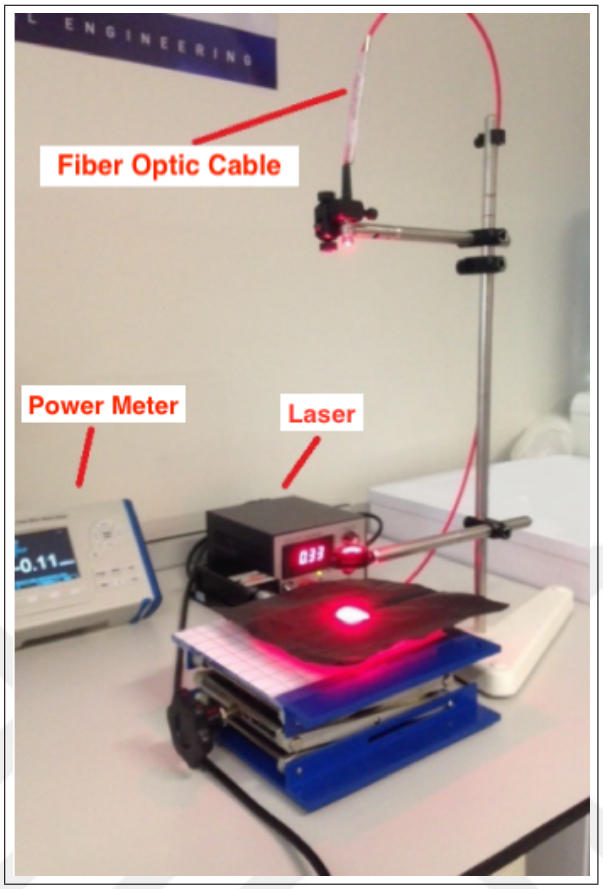

Figure 5.1 Experimental Setup of the Laser System

5.4 Preparation of Au-ICG NPs

Gold nanoparticles used as core were purchased ready (Sigma-Aldrich, 741981, 40 nm). The procedure for coating these nanoparticles with PEI (Polyethylenimine, Linear, MW 25,000 (PEI 25000), Polysciences 23966-1) and ICG was adapted from the corresponding article of Kuo et al [30].

In order to optimize the concentration of the solutions to be used for the coating, at first the gold suspension diluted with a constant amount of 1:2 pure water was mixed with different concentrations of PEI solution, and the zeta potentials of the obtained PEI coated nanoparticles were measured and the concentration at which they were coated with the most PEI was determined.

Then, 50 μM ICG solution was mixed with PEI coated gold nanoparticles at different volume ratios and again using zeta potential measurements, the volume ratios enabling maximum binding of ICG on nanoparticles were determined.

In order to produce the nanoparticles to be used for PDT experiments;

1. The gold suspension was first diluted to a volume of 1:2 gold suspension/ultrapure water and the nanoparticles were dispersed homogenously by an ultrasonic homogenizer.
2. The particles were then mixed together with a 1% solution of PEI in methanol for 2 hours to form the PEI coating and then the particles were precipitated by centrifugation and washed twice with methanol.
3. After the addition of 50 μM ICG stock solution for ICG coating, the nanoparticles were stirred for an additional 2 hours and again precipitated by centrifugation. The supernatant was taken to determine the amount of ICG bounded and the particles were washed 2 times with ultrapure water.

5.5 Characterization of Au-ICG NPs

The size and zeta potential measurements of nanoparticles were obtained by Dynamic Light Scattering (DLS) method using Brookhaven 90Plus Nanoparticle Size / Zeta Potential Analyzer.

Scanning Electron Microscope (SEM) images obtained by using the Philips-FEI XL30 ESEM-FEG Scanning Electron Microscope to investigate particle morphology.

Figure 5.2 Initial ICG solution and the supernatant after ICG conjugation.

After ICG loading was completed, the nanoparticles were precipitated by centrifugation, the amount of unbound ICG remaining in the supernatant was calculated based on a calibration curve previously prepared by the colorimetric method. The calibration curve and equation used for this purpose are given in Figure 5.3. The amount of bounded ICG was calculated by subtracting the concentration of the supernatant from the initial ICG concentration.

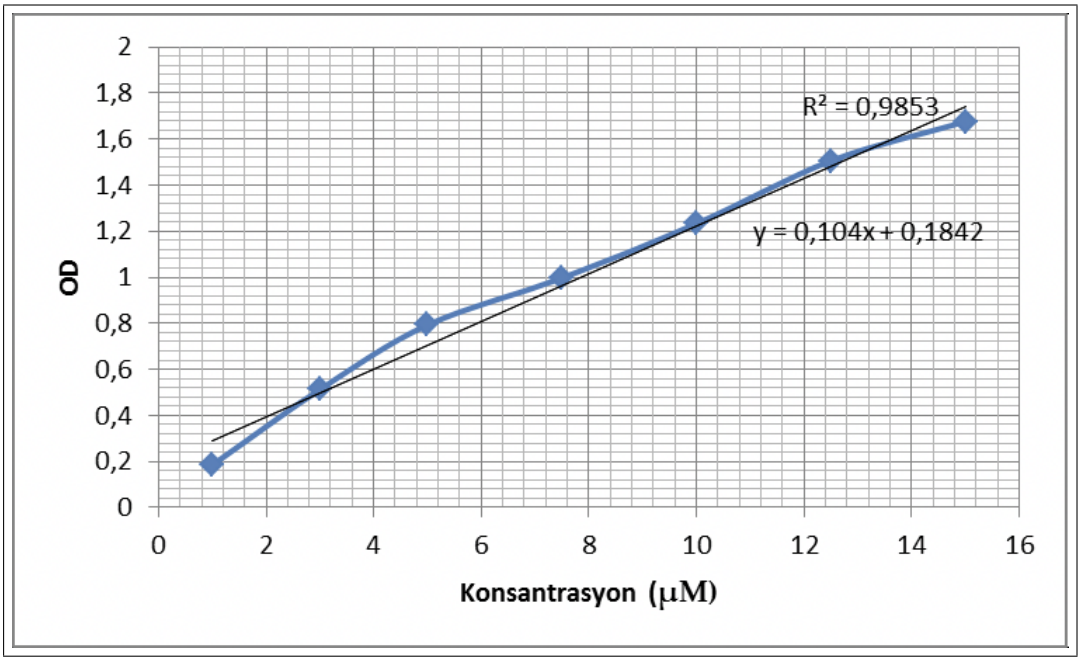

Figure 5.3 ICG calibration curve in water.

The singlet oxygen quenching property of DPBF (1,3-Diphenylisobenzofuran) was used to determine the singlet oxygen production capacity of nanoparticles. In this method, solutions containing certain amounts of PS and DPBF are irradiated at certain intervals (20s) at a specific laser power density (100 mW / cm2). When ICG interacts with laser and starts to produce singlet oxygen, DBPF in the environment interacts with singlet oxygen, causing the absorbance peak of DBPF to decrease. Naturally, DBPF is a yellow chemical with absorbance at 410 nm, but it becomes transparent if interacts with singlet oxygen. The time-DPBF absorption curve obtained from irradiations can be used to calculate the singlet oxygen quantum efficiency using the following formula. Methylene blue (MB) was used as the standard for singlet oxygen quantum efficiency calculation. The yield was calculated by comparing the slope of the decrease in the absorbance peak of DPBF caused by ICG to the slope formed by the MB singlet oxygen yield.

$$\Phi(^1O_2)^{NP} = \Phi(^1O_2)^{MB} \frac{m^{NP} F^{NP}}{m^{MB} F^{NP}} \tag{5.1}$$

5.6 PDT application

The method of PDT applications with ICG and AuNP-ICG is as follows;

1. Cells that reached a sufficient number for PDT administration were first removed by trypsinization, counted, and seeded in 96-well plates with 15,000 cells per well.
2. The cultivated cells were incubated for 24 hours and allowed to attach to the surface.
3. Subsequently, cells medium exchanged with the medium containing the corresponding PS, then they were incubated for a further 2 hours.
4. At the end of 2 hours, the medium containing PS was replaced with fresh medium and laser irradiation was applied to the wells at determined doses.

Each experiment was repeated at least 3 times.

5.7 Determination of cytotoxicity by MTT test

10 μL of 5 mg / mL MTT solution was added to the plates which were incubated for 24 hours after PDT application and incubated for a further 3 hours at 37 $^{\circ}$C and the wells were emptied after 3 hours. The resulting formazan crystals were dissolved in 100 μl of DMSO and the absorbance at 570 nm was read in the microplate reader.

5.8 Statistical Analysis

Cell viability data obtained after three independent analyzes for each experimental group were first normalized with the help of control groups. Then, the mean and standard deviation values of each group were compared with each other using ANOVA and Tukey tests (significance level 5% ($p \leq 0.05$)).

6. RESULTS

6.1 Characterization of NPs

To determine the ratio required for Au NPs to be coated with sufficient amount of PEI, different ratios of (AuNP:PEI, 1:0.005, 1:0.1, 1:0.25, 1:0.5, 1:1) AuNP and PEI were mixed and then zeta potential measured after coating.

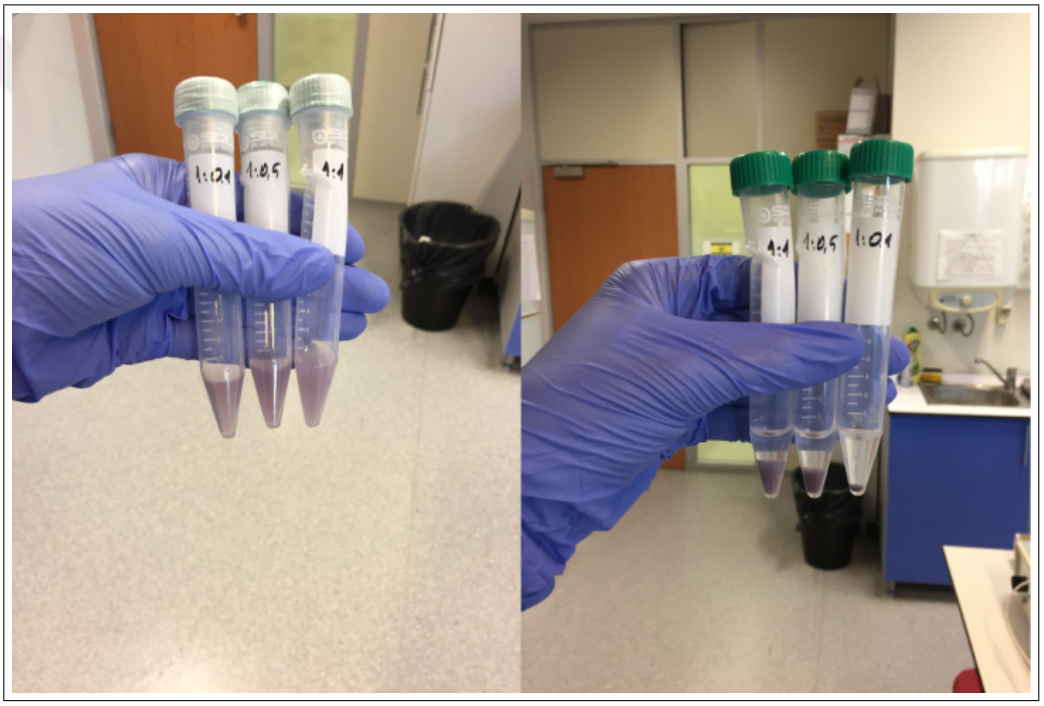

Figure 6.1 Au-PEI NPs before and after centrifugation.

To determine the ratio required for AuPEIs to be coated with an adequate amount of ICG, zeta potentials were measured with different ratios (Au:ICG, 1:0.5, 1:1, 1:1.5).

The DLS size and zeta potential measurements of the nanoprecipitates obtained are given in the table 6.1.

According to the results given in Table 6.1, we can observe the successful loading of PEI molecules on AuNP with increasing zeta potential. In the measurements taken to

Table 6.1
AuNP Zeta Potential and DLS measurements.

Sample	**Zeta Pot(mV)**	**Std Error**	**Size (nm)**
AuNP	-19.25	2.42	66.2
AuPEI 1:0.05	49.44	0.67	
AuPEI 1:0.1	50.74	0.73	
AuPEI 1:0.25	56.65	1.95	
AuPEI 1:0.5	58.47	2.18	
AuPEI 1:1	61.13	0.79	73.2
AuICG 1:0.5	-22.23	0.77	
AuICG 1:1	-29.91	0.65	216.7
AuICG 1:1.5	-30.27	0.54	178.1
AuICG-1	-7.33	0.96	173.8

determine the AuNP: PEI ratio, the highest zeta potential was measured at a 1:1 ratio, although a significant increase in zeta potential was not observed by increasing the PEI amount. The 1:1 ratio provided sufficient coating and was used in the experiments. We can observe that ICG coating was also successful in the decrease of zeta potential of AuICG NPs. The same route was used to determine the Au:ICG ratio required for sufficient ICG coating of AuPEI NPs. It was observed that for 1:1 and 1:1.5 ratios more ICG loading occurred compared to 1:0.5 ratio. Since there was not much difference between the 1:1 and 1:1.5 ratios, the 1:1 ratio was preferred considering that ICG aggregation would be less at low concentrations. AuICG DLS measurements were then used to check whether the particles were suitable for intracellular uptake. Particles having an average size of 180.76 nm are suitable for intracellular uptake.

The resulting nanoparticles were dried on aluminum foil and SEM images were taken. Drying was carried out by leaving samples in an incubator at 38 $^{\circ}$C overnight in the dark. In SEM images (Figure 6.2) taken to investigate the morphology of the particles, the coating around the NPs, which is formed by multiple AuNPs, is observed as a cloudy layer. While the gold nuclei can be observed as bright spots

of approximately 40 nm in size from the Figure 6.2 C and D, the boundaries of the PEI-ICG sheath covering them are observed as a more weak and cloudy structure. The obtained clusters gave similar results to the size measurements taken by DLS method as average size.

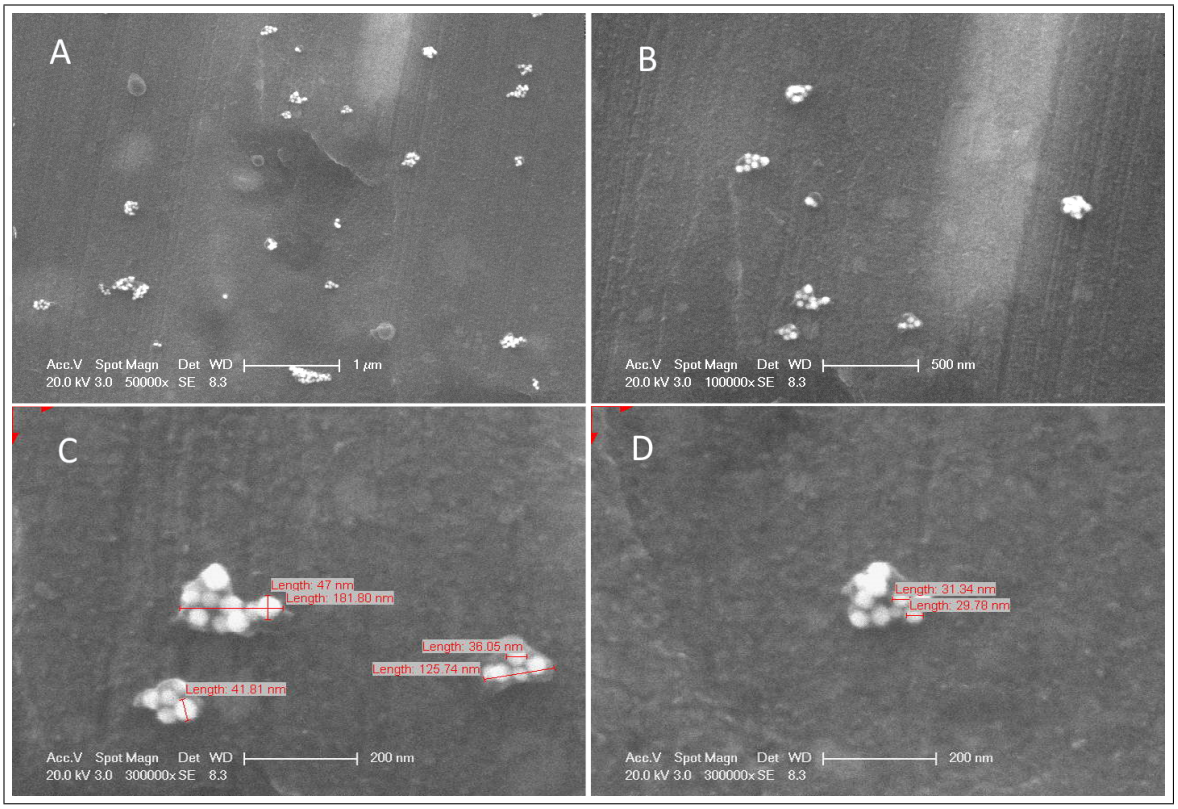

Figure 6.2 SEM images of AuICG NPs.

These clusters are prepared to be used for PDT application in the cell, as it is observed that the three nanoparticles produced as a result of the final procedure have the same properties in three replications.

The data obtained from the absorption measurements of MB and AuICG which were performed in order to calculate the singlet oxygen production efficiency of the prepared particles are shown in Figure 6.3.

As a result of the calculations made with the Equation 6.1, it is seen that the particles singlet oxygen quantum efficiency of nanoprecipitates is 0.0025.

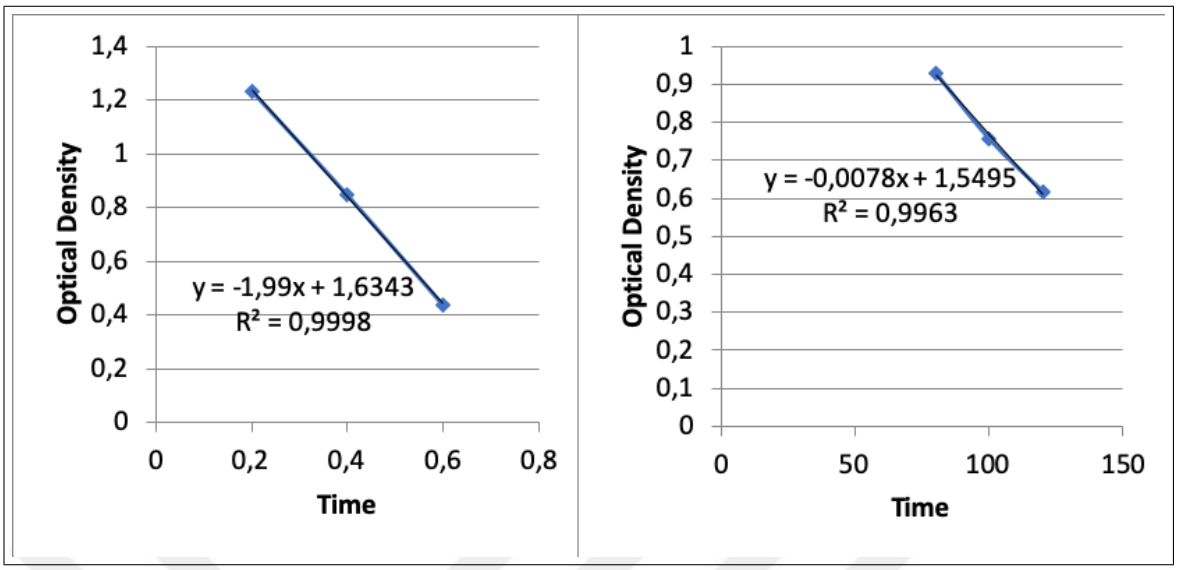

Figure 6.3 Absorption measurements of MB (635 nm) and AuICG (809 nm) in DPBF solution.

$$\Phi('O_2)_{AuICG} = \Phi('O_2)_{MB} \cdot \frac{m^{AuICG}}{m^{MB}} \cdot \frac{F^{MB}}{F^{AuICG}} \qquad (6.1)$$
$$\Phi('O_2)_{AuICG} = 0.0025$$

6.2 PDT Application

6.2.1 PDT Applications on Caco-2 Cell Line

The effects of the prepared nanoparticles in different ICG and laser doses in the Caco-2 cell line are shown in the following results.

From the graph in the Figure 6.4, it is observed that the Au NPs carrying 50 μM ICG have low PDT activity. When the nanoparticle groups were compared with the no-treatment group, it can be seen that cell viability decreased. However, this decrease is not valuable because it also means that AuICG NPs have dark toxicity (26% decrease in cell viability).

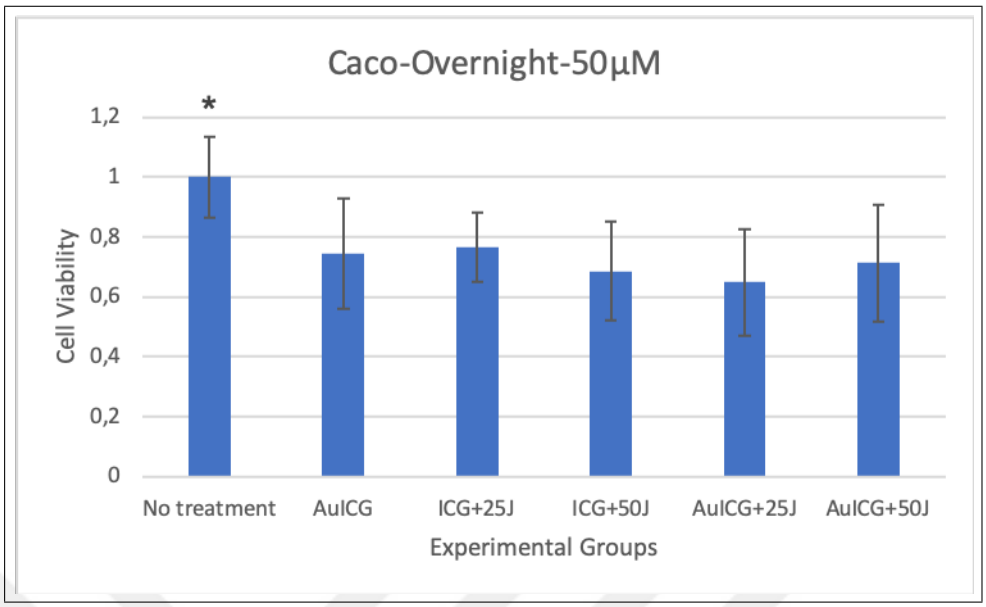

Figure 6.4 MTT results of the PDT on Caco-2 cell line with 50 μM ICG concentration. 25 and 50 J/cm^2 laser energy densities effects were tested. In these treatment sessions, PSs were incubated overnight. No treatment group significantly different from the rest of the groups.

In Figure 6.5, only AuICG irradiated with 100 J/cm^2 power density showed a significant difference compared to the control group. This indicates that the PDT effectiveness of NPs could be increased along with the laser power density increase.

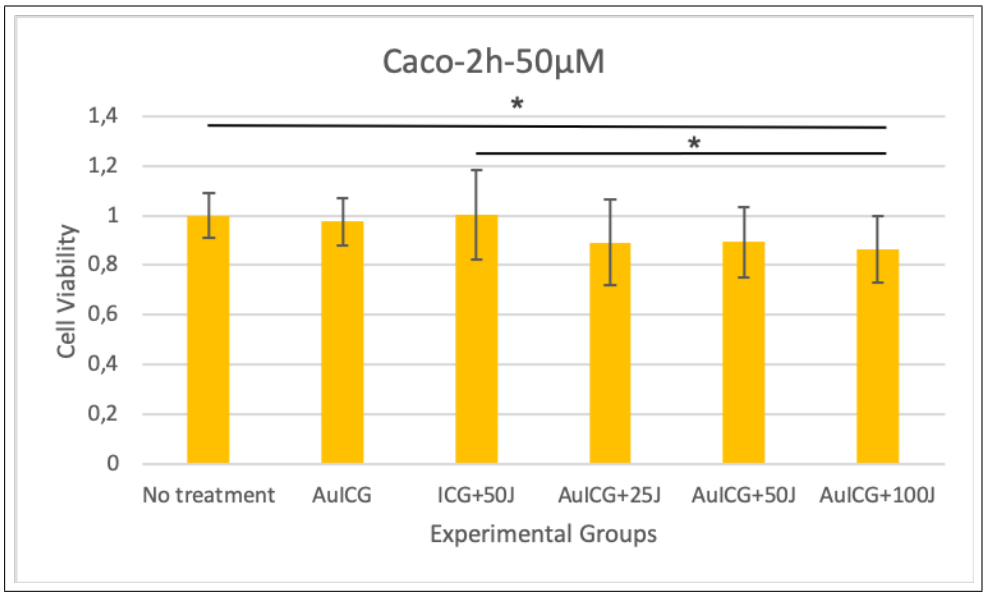

Figure 6.5 MTT results of the PDT on Caco-2 cell line with 50 μM ICG concentration. 25, 50 and 100 J/cm^2 laser energy densities effects were tested. In these treatment sessions, PSs were incubated for 2 hours. Groups at each end of the sticks significantly different from each other.

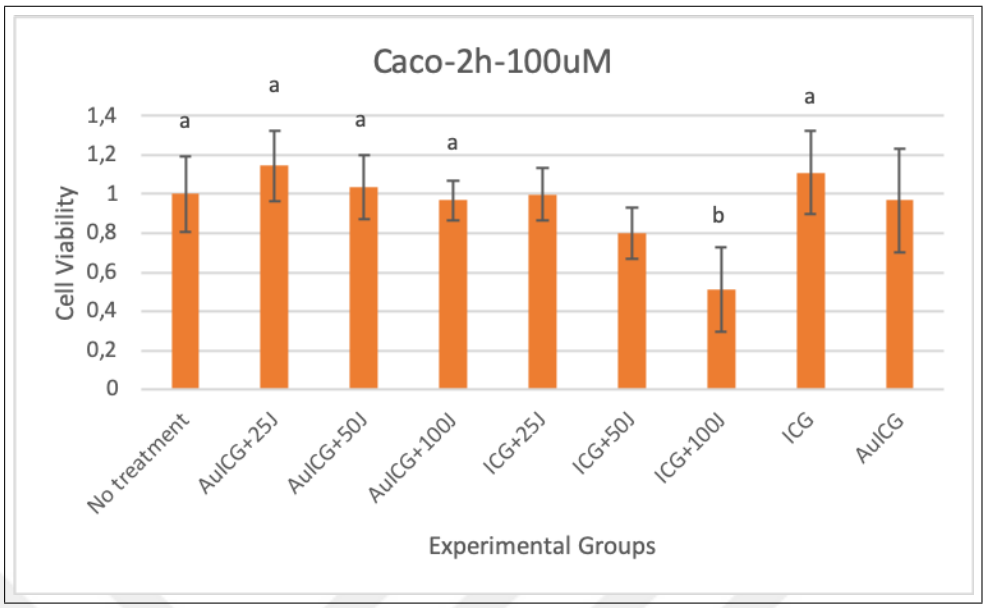

Figure 6.6 MTT results of the PDT on Caco-2 cell line with 100 μM ICG concentration. 25, 50 and 100 J/cm^2 laser energy densities effects were tested. In these treatment sessions, PSs were incubated for 2 hours. ICG+100J group is significantly different from the groups labeled with "a" letter.

In nanoparticles carrying 100 μM ICG (Figure 6.6), an increase in cell viability was observed when laser irradiation was performed, but this increase was not statistically significant. Compared with free ICG, AuICG groups had lower PDT activity than free ICG groups in general. Especially, ICG+100J showed remarkable PDT activity by decreasing cell viability to 51%.

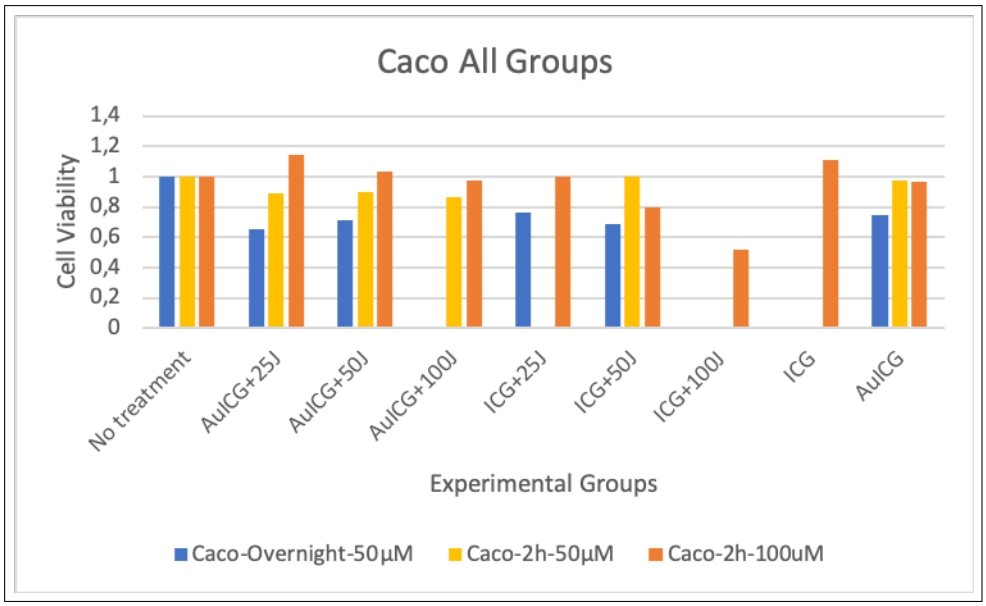

Figure 6.7 Combinatory graph of the treatment groups on the Caco-2 cell line.

Table 6.2
Comparison of all Caco-2 groups. Means that do not share a letter are significantly different.

Treatment	**Grouping**
3-AuICG+25J	A
3-ICG	A B
3-AuICG+50J	A B C
2-ICG+50J	A B C
1-No treatment	A B C D
2-No treatment	A B C
3-No treatment	A B C
3-ICG+25J	A B C D
2-AuICG	A B C D
3-AuICG+100J	A B C D E
3-AuICG	A B C D E
2-AuICG+50J	B C D E F
2-AuICG+25J	C D E F
2-AuICG+100J	C D E F G
3-ICG+50J	C D E F G
1-ICG+25J	D E F G
1-AuICG	E F G H

According to Caco-2 results (Figure 6.7), there is low dark toxicity of nanoparticles for Caco-2 cell line. In 50 μM AuICG groups with no laser irradiation, there is a significant difference between 2h and overnight incubation. Overnight incubation increases the dark toxicity of NPs. For AuICG irradiated with 25 J/cm^2 power density, it can be said that the effectiveness of PDT increases with the ICG concentration.

6.2.2 PDT Applications on PC-3 Cell Line

The effects of the prepared nanoparticles in different ICG and laser doses in the PC-3 cell line are shown in the following results.

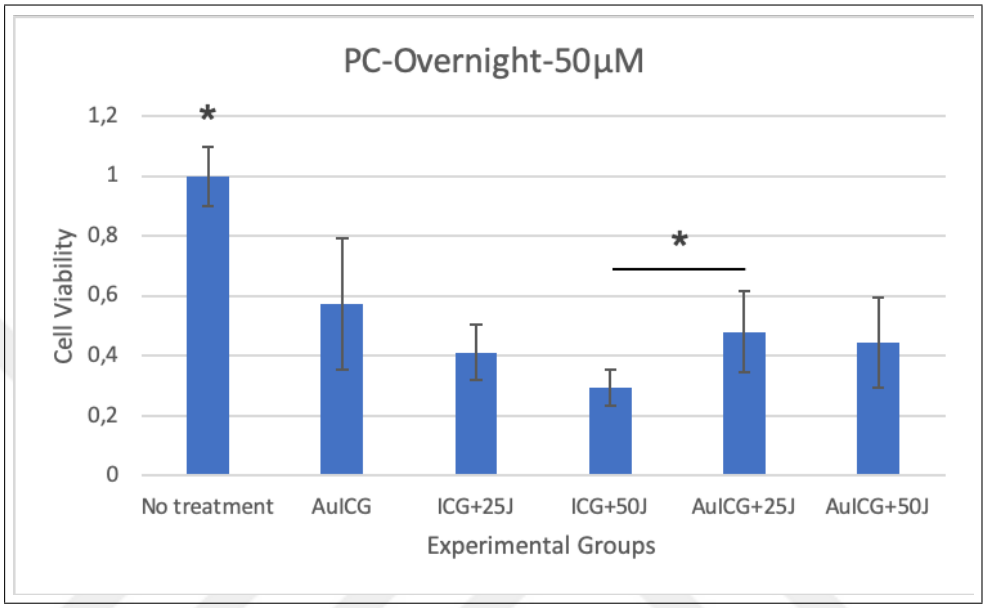

Figure 6.8 MTT results of the PDT on PC-3 cell line with 50 μM ICG concentration. 25 and 50 J/cm^2 laser energy densities effects were tested. In these treatment sessions, PSs were incubated overnight. No treatment group significantly different from the rest of the groups. ICG+50J and AuICG+25J showed a significant difference from each other.

In Figure 6.8, no treatment group significantly different from all other groups meaning that there is a notable viability decrease with all treatments but it originates mostly from dark toxicity (43% cell viability decrease).

From the graph shown in Figure 6.9 it is observed that the Au NPs carrying 50 μM ICG have a notable impact on cell viability. However, this decrease is not valuable because it also means that AuICG NPs have dark toxicity (32% decrease in cell viability).

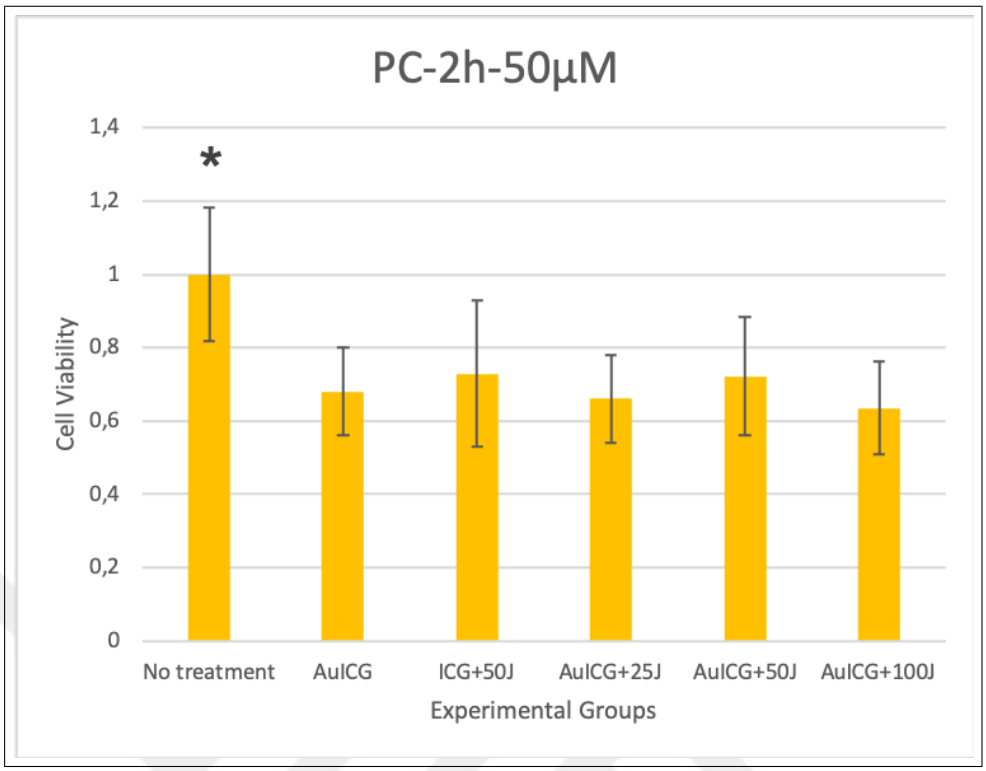

Figure 6.9 MTT results of the PDT on PC-3 cell line with 50 μM ICG concentration. 25, 50 and 100 J/cm^2 laser energy densities effects were tested. In these treatment sessions, PSs were incubated for 2 hours. No treatment group significantly different from the rest of the groups.

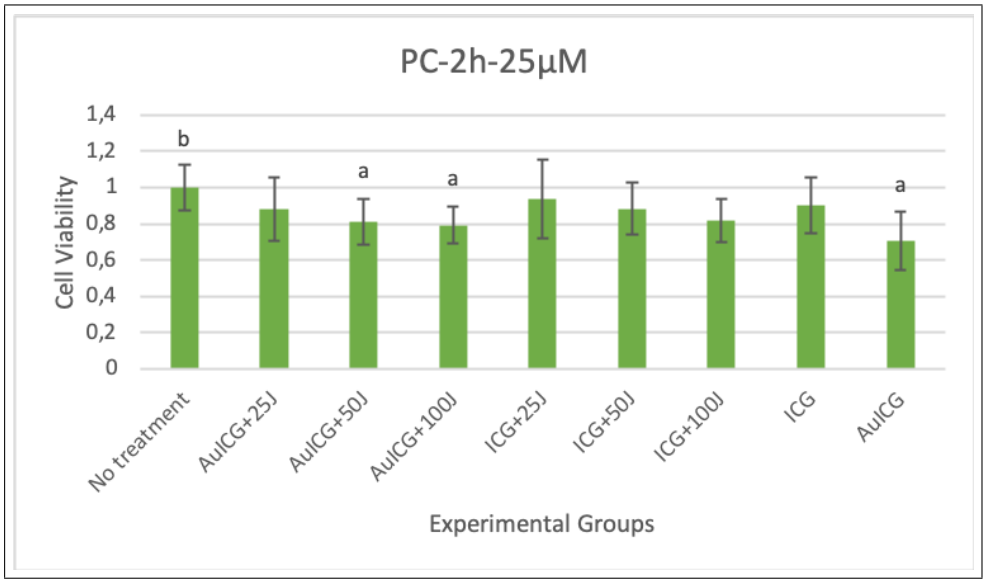

Figure 6.10 MTT results of the PDT on PC-3 cell line with 25 μM ICG concentration. 25, 50 and 100 J/cm^2 laser energy densities effects were tested. In these treatment sessions, PSs were incubated for 2 hours. No treatment group significantly different from the groups labeled with "a" letter.

The graph on Figure 6.10 shows that there is a notable cell viability drop with

the treatment using NPs for higher laser doses. However, it is not due to PDT activity but from dark toxicity (29% cell viability decrease).

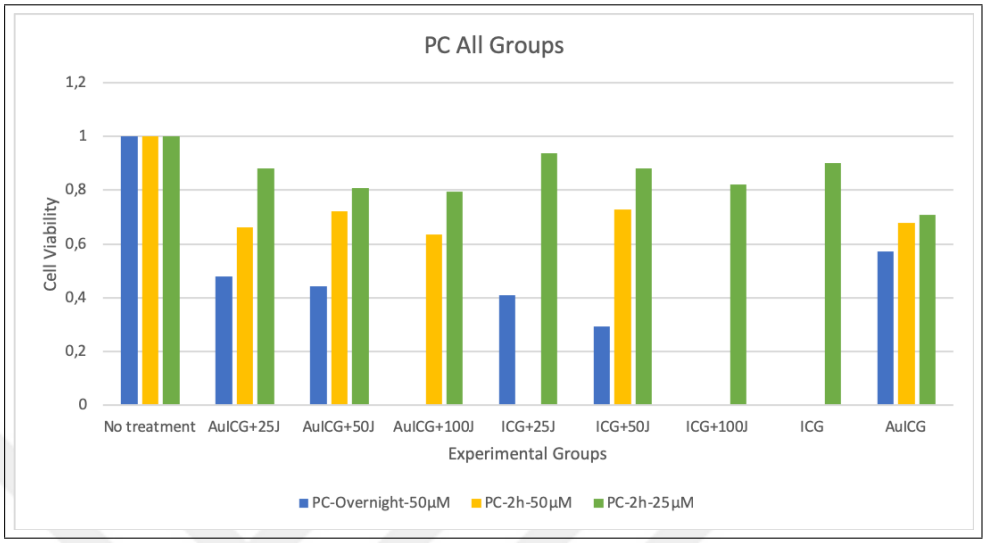

Figure 6.11 Combinatory graph of the treatment groups on the PC-3 cell line.

PDT results for the PC-3 cell line are summarized in the Figure 6.11. According to these results, the dark toxicity of AuICG nanoparticles is higher than the results obtained in Caco-2, therefore no doses higher than 50 μM were tested for PDT applications. Although the PDT activity of AuICG for the PC-3 cell line was observed to be slightly better than that of free ICG at all tested doses, there is no statistical significance of this difference. Furthermore, no significant difference was observed between PDT groups and dark toxicity when these groups were compared with dark toxicity. Therefore, the decrease in cell viability is thought to be the result of toxicity rather than PDT activity. For all AuICG irradiated with 25 and 100 J/cm^2 power density groups, it can be said that the effectiveness of PDT increases with the ICG concentration.

Table 6.3
Comparison of all PC-3 groups. Means that do not share a letter are significantly different.

Treatment	**Grouping**
1-No treatment	A
3-No treatment	A B
3-ICG+25J	A B
3-ICG	A B C
1-No treatment	A B C
3-AuICG+25J	A B C
3-ICG+50J	A B C
3-ICG+100J	A B C D
3-AuICG+50J	A B C D E
3-AuICG+100J	B C D E F
3-AuICG	C D E F G
2-ICG+50J	D E F G H
2-AuICG+50J	D E F G H
2-AuICG	D E F G H I
2-AuICG+25J	E F G H I
1-AuICG	F G H I
2-AuICG+100J	G H I
1-AuICG+25J	G H I J
1-AuICG+50J	H I J
1-ICG+25J	I J
1-ICG+50J	J

7. DISCUSSION

PDT is an advantageous treatment with its minimally invasive, repeatable treatment and selective toxic effects on cancer cells properties. ICG is an FDA approved, non-toxic dye with a strong absorption peak in the near-infrared region in the electromagnetic spectrum. However, aggregation and high protein binding tendencies limit the use of aqueous solutions of ICG due to their relatively unstable nature.

ICG-PDT has previously been shown to affect cell viability in colon and prostate cancer cells in a dose-dependent way. However, PC-3 was more susceptible to ICG-PDT, whereas the Caco-2 cell line was more resistant [35].

In this study, the effects of ICG on gold nanoparticles and PDT application in the same cell lines were investigated. Several studies have reported that nanoparticle drug delivery systems increase ICG's photo and thermal stability, prevent aggregation and binding to serum proteins, and increase circulation time [36][37].

Primarily, it was aimed to load ICG with the help of PEI on 40 nm AuNPs and characterize the obtained particles. The negatively charged surface of Au NPs are coated with positively charged PEI and the negatively charged ICG is attached by electrostatic interaction. Raise of the zeta potential indicated that PEI molecules were successfully loaded onto Au NPs. We were also able to observe that the ICG coating was also successful due to the decrease in zeta potential in AuICG NPs. Afterward, in the SEM images, it was found that Au NPs were coated as clusters. In AuICG DLS measurements, it was found that particles having a mean size of 180,76 nm, although they were coated in clustered form, were suitable for intracellular uptake. Since singlet oxygen production of the NPs is an essential factor in the effectiveness of PDT, singlet oxygen production efficiency was evaluated too. As a result of the calculations, it was seen that the particles produced enough singlet oxygen when irradiated with 809 nm laser to show PDT activity.

To investigate the changes in PDT effectiveness on Caco-2 and PC-3 cell lines using ICG loaded Au NPs MTT tests were carried out. As a result of the MTT tests, the particles were found to be toxic even without laser interaction. This is likely due to the high concentration of PEI used as a binding molecule. If the AuNPs are overcoated with PEI and the ICG is not completely covered by PEI, PEI may cause toxic effects in the cell.

In the literature, studies on AuICG are small in number and include particles of different morphologies (nanoparticles, nanorods, etc.). However, in these studies, the surface plasmon resonances of the gold nanostructures were generally adjusted considering the absorption maximum of ICG. In this way, photothermal effects were also utilized. However, this makes difficult to compare this study with AuICG studies in the literature [30][38][39]. Since the absorption maxima of the 40 nm diameter gold nanoparticles used in this study are around 530 nm, they do not interfere with the laser radiation of 809 nm, so no thermal effect from the plasmon resonance of the nanoparticles is observed. In the study of Kuo et al., the synergistic effect of PDT and PTT was utilized and effective results were obtained. In addition, Kuo et al. showed that conjugation of AuICG NPs with anti-epidermal growth factor increased PDT efficiency compared to AuICG alone [30]. The absence of a targeting molecule in this study may also limit the efficacy of PDT.

However, it has been seen that free ICG can produce much more singlet oxygen than AuICG. It has recently been found in the literature that direct contact of photosensitizers with gold surfaces directly affects singlet oxygen production [18]. This difference can be used to explain the low efficiency of AuICG-PDT. Therefore, it can be thought that the reason of the presence of gold as a good ICG carrier in the literature is that the absorption properties of local SPR rather than photodynamic effects. In this study, we aimed to focus on only PDT properties of AuICG's thus the effect was very low.

Results from cell viability also show a variable sensitivity in ICG-based treatment between the studied cell lines. The sensitivity difference could be originated

from the grade of cancer and structural differences. Moesta et al. found that different grades of pancreatic cancer cells react differently to PDT [40]. Lower graded cancer cells show less photodynamic therapy effects as these cells have improved survival strategies. These cells are also called well-differentiated cells. Likewise, in our experiments, well-differentiated Caco-2 cells affected less unlike badly differentiated PC-3 cells [35].

Based on these results, AuICG NPs, in which PEI is used as a binder, have been observed to be a suitable carrier for ICG, but PDT activity is very low and dark toxicity presents at high doses. However, gold nanoparticles are still a promising carrier for combined PDT/PTT treatments. Nonetheless, the high cell killing ability observed in such treatments may be thought to be due to photothermal effects rather than photodynamic effects.

8. CONCLUSION

The PDT approach for clinical cancer therapy is a well-established, minimally invasive and not toxic method. In comparison with other treatment techniques like surgery, chemotherapy, and radiation treatment, PDT treatment has comparatively fewer side effects, quick patient recovery and is easier to administer.

The development of new photosensitizers appropriate for the therapy of deeper tissue tumors is a serious challenge in PDT therapy. ICG is highly absorbed by 800 nm, thus can penetrate into the tissue comparatively deeply. Unfortunately, ICG has very low water solubility and low stability in its aqueous solutions, and it has a tendency to form strong bonds with plasma proteins. In order to overcome these disadvantages, the transportation of ICG with gold nanoparticles was studied in this thesis.

As a result of the MTT tests, the particles were found to have dark toxicity. This is probably because of the high levels of PEI used as a binding molecule. To overcome this problem, short-chain PEI molecules of lower molecular weight may be preferred to reduce the toxic effect. Using a different binder polymer can also be considered as an alternative solution.

In the study of Kuo et al., the synergistic effect of PDT and PTT observed and effective results were obtained. In addition, Kuo et al. Showed that conjugation of AuICG particles with anti-epidermal growth factor increased PDT efficiency compared to AuICG alone [30]. In further studies, the results obtained in this thesis can be compared with a therapy using a targeting molecule attached to AuICG NPs to determine the effect of targeting. In addition, the PTT efficiency of the particles can be tested by increasing the power density and application time.

As a result, in this study, characterization of ICG loaded gold nanoparticles was completed by performing zeta potential and size measurements, the efficiency of

PDT was investigated by MTT tests and the particles were observed to be toxic. In future studies, an effective PDT can be achieved by solving the toxicity problem, using targeting molecules and taking advantage of photothermal effects.

REFERENCES

1. Beik, J., M. Khateri, Z. Khosravi, S. K. Kamrava, S. Kooranifar, H. Ghaznavi, and A. Shakeri-Zadeh, "Gold nanoparticles in combinatorial cancer therapy strategies," *Coordination Chemistry Reviews*, Vol. 387, pp. 299–324, 2019.

2. Nygren, P., "What is cancer chemotherapy?," *Acta Oncologica*, Vol. 40, no. 2-3, pp. 166–174, 2001.

3. Agostinis, P., K. Berg, K. A. Cengel, T. H. Foster, A. W. Girotti, S. O. Gollnick, S. M. Hahn, M. R. Hamblin, A. Juzeniene, and D. Kessel, "Photodynamic Therapy of Cancer: An Update," *Ca Cancer J Clin*, Vol. 61, no. April, pp. 250–281, 2017.

4. Philip, R., A. Penzkofer, W. Bäumler, R. Szeimies, and C. Abels, "Absorption and fluorescence spectroscopic investigation of indocyanine green," *Journal of Photochemistry and Photobiology A: Chemistry*, Vol. 96, no. 1-3, pp. 137–148, 1996.

5. Abels, C., M. Mauerer, W. Holzer, M. Landthaler, W. Bäumler, A. Penzkofer, and R.-M. Szeimies, "Photostability and thermal stability of indocyanine green," *Journal of Photochemistry and Photobiology B: Biology*, Vol. 47, no. 2-3, pp. 155–164, 2002.

6. Gomes, A. J., L. O. Lunardi, J. M. Marchetti, C. N. Lunardi, and A. C. Tedesco, "Indocyanine green nanoparticles useful for photomedicine," *Photomedicine and Laser Therapy*, Vol. 24, no. 4, pp. 514–521, 2006.

7. Manchanda, R., A. Fernandez-Fernandez, A. Nagesetti, and A. J. McGoron, "Preparation and characterization of a polymeric (PLGA) nanoparticulate drug delivery system with simultaneous incorporation of chemotherapeutic and thermo-optical agents," *Colloids and Surfaces B: Biointerfaces*, Vol. 75, no. 1, pp. 260–267, 2010.

8. "What is cancer?," *National Cancer Institute*.

9. Eldridge, L., "Cancer cells vs. normal cells: How are they different?," *Verywell Health*.

10. Cooper, G. M., *The Cell: A Molecular Approach. 2nd edition.*, Sinauer Associates, 2000.

11. American Cancer Society, "Facts & Figures 2019," tech. rep., Atlanta, 2019.

12. Haggar, F. A., and R. P. Boushey, "Colorectal cancer epidemiology: Incidence, mortality, survival, and risk factors," *Clinics in Colon and Rectal Surgery*, Vol. 22, no. 4, pp. 191–197, 2009.

13. Siddiqui, L., H. Mishra, P. K. Mishra, Z. Iqbal, and S. Talegaonkar, "Novel 4-in-1 strategy to combat colon cancer, drug resistance and cancer relapse utilizing functionalized bioinspiring lignin nanoparticle," *Medical Hypotheses*, Vol. 121, no. July, pp. 10–14, 2018.

14. Dunn, M. W., N. Practitioner, C. Hill, A. N. Practitioner, and L. Comprehensive, "Prostate cancer review," Vol. 27, no. 4, pp. 241–250, 2011.

15. Lucky, S. S., K. C. Soo, and Y. Zhang, "Nanoparticles in Photodynamic Therapy," *Chemical Reviews*, Vol. 115, no. 4, pp. 1990–2042, 2015.

16. Kelly, J., and M. Snell, "Hematoporphyrin derivative: a possible aid in the diagnosis and therapy of carcinoma of the bladder," *The Journal of urology*, Vol. 115, no. 2, pp. 150–151, 1976.

17. Dougherty, T. J., J. E. Kaufman, A. Goldfarb, K. R. Weishaupt, D. Boyle, and A. Mittleman, "Photoradiation therapy for the treatment of malignant tumors," *Cancer research*, Vol. 38, no. 8, pp. 2628–2635, 1978.

18. Shirata, C., J. Kaneko, Y. Inagaki, T. Kokudo, M. Sato, S. Kiritani, N. Akamatsu, J. Arita, Y. Sakamoto, K. Hasegawa, and N. Kokudo, "Near-infrared photothermal/photodynamic therapy with indocyanine green induces apoptosis of hepatocellular carcinoma cells through oxidative stress," *Scientific Reports*, Vol. 7, no. 1, pp. 1–8, 2017.

19. Castano, A. P., T. N. Demidova, and M. R. Hamblin, "Mechanisms in photodynamic therapy: part one—photosensitizers, photochemistry and cellular localization," *Photodiagnosis and photodynamic therapy*, Vol. 1, no. 4, pp. 279–293, 2004.

20. Bakhmetyev, V. V., T. S. Minakova, S. V. Mjakin, L. A. Lebedev, A. B. Vlasenko, A. A. Nikandrova, I. A. Ekimova, N. S. Eremina, M. M. Sychov, and A. Ringuede, "Synthesis and surface characterization of nanosized y2o3: Eu and yag: Eu luminescent phosphors which are useful in photodynamic therapy of cancer," *European Journal of Nanomedicine*, Vol. 8, no. 4, pp. 173–184, 2016.

21. Josefsen, L. B., and R. W. Boyle, "Photodynamic Therapy and the Development of Metal-Based Photosensitisers," *Metal-Based Drugs*, Vol. 2008, pp. 1–23, 2008.

22. Avci, P., A. Gupta, M. Sadasivam, D. Vecchio, Z. Pam, N. Pam, and M. R. Hamblin, "Low-level laser (light) therapy (lllt) in skin: stimulating, healing, restoring," in *Seminars in cutaneous medicine and surgery*, Vol. 32, p. 41, NIH Public Access, 2013.

23. Svanberg, K., and N. Bendsoe, "Photodynamic therapy for human malignancies with superficial and interstitial illumination," in *Lasers for Medical Applications*, pp. 760–778, Elsevier, 2013.

24. Giraudeau, C., A. Moussaron, A. Stallivieri, S. Mordon, and C. Frochot, "Indocyanine Green: Photosensitizer or Chromophore? Still a Debate," *Current Medicinal Chemistry*, Vol. 21, no. 16, pp. 1871–1897, 2014.

25. Ghorbani, F., N. Attaran-Kakhki, and A. Sazgarnia, "The synergistic effect of photodynamic therapy and photothermal therapy in the presence of gold-gold sulfide nanoshells conjugated Indocyanine green on HeLa cells," *Photodiagnosis and Photodynamic Therapy*, Vol. 17, pp. 48–55, 2017.

26. Sanna, V., N. Pala, and M. Sechi, "Targeted therapy using nanotechnology: focus on cancer," *International journal of nanomedicine*, Vol. 9, p. 467, 2014.

27. Gurunathan, S., M.-H. Kang, M. Qasim, and J.-H. Kim, "Nanoparticle-Mediated Combination Therapy: Two-in-One Approach for Cancer.," *International journal of molecular sciences*, Vol. 19, no. 10, pp. 1–37, 2018.

28. Fang, S., C. Li, J. Lin, H. Zhu, D. Cui, Y. Xu, and Z. Li, "Gold nanorods-based theranostics for simultaneous fluorescence/two-photon luminescence imaging and synergistic phototherapies," *Journal of Nanomaterials*, Vol. 2016, p. 1, 2016.

29. Kuo, W. S., C. N. Chang, Y. T. Chang, M. H. Yang, Y. H. Chien, S. J. Chen, and C. S. Yeh, "Gold nanorods in photodynamic therapy, as hyperthermia agents, and in near-infrared optical imaging," *Angewandte Chemie - International Edition*, Vol. 49, no. 15, pp. 2711–2715, 2010.

30. Kuo, W., Y. Chang, K. Cho, K. Chiu, C. Lien, C. Yeh, and S. Chen, "Biomaterials Gold nanomaterials conjugated with indocyanine green for dual-modality photodynamic and photothermal therapy," *Biomaterials*, Vol. 33, no. 11, pp. 3270–3278, 2012.

31. Cui, H., D. Hu, J. Zhang, G. Gao, Z. Chen, W. Li, P. Gong, Z. Sheng, and L. Cai, "Gold nanoclusters–indocyanine green nanoprobes for synchronous cancer imaging, treatment, and real-time monitoring based on fluorescence resonance energy transfer," *ACS applied materials & interfaces*, Vol. 9, no. 30, pp. 25114–25127, 2017.

32. Li, W., H. Zhang, X. Guo, Z. Wang, F. Kong, L. Luo, Q. Li, C. Zhu, J. Yang, Y. Lou, *et al.*, "Gold nanospheres-stabilized indocyanine green as a synchronous photodynamic–photothermal therapy platform that inhibits tumor growth and metastasis," *ACS applied materials & interfaces*, Vol. 9, no. 4, pp. 3354–3367, 2017.

33. Liu, F., Y. Zhang, S. Liu, B. Zhang, Q. Liu, Y. Yang, J. Luo, B. Shan, and J. Bai, "Monitoring of tumor response to au nanorod-indocyanine green conjugates mediated therapy with fluorescence imaging and positron emission tomography," *IEEE Transactions on Multimedia*, Vol. 15, no. 5, pp. 1025–1030, 2013.

34. Luo, T., X. Qian, Z. Lu, Y. Shi, Z. Yao, X. Chai, and Q. Ren, "Indocyanine green derivative covalently conjugated with gold nanorods for multimodal phototherapy of fibrosarcoma cells," *Journal of biomedical nanotechnology*, Vol. 11, no. 4, pp. 600–612, 2015.

35. Ruhi, M. K., A. Ak, and M. Gülsoy, "Dose-dependent photochemical/photothermal toxicity of indocyanine green-based therapy on three different cancer cell lines," *Photodiagnosis and photodynamic therapy*, Vol. 21, pp. 334–343, 2018.

36. Saxena, V., M. Sadoqi, and J. Shao, "Indocyanine green-loaded biodegradable nanoparticles: preparation, physicochemical characterization and in vitro release," *International journal of pharmaceutics*, Vol. 278, no. 2, pp. 293–301, 2004.

37. Saxena, V., M. Sadoqi, and J. Shao, "Enhanced photo-stability, thermal-stability and aqueous-stability of indocyanine green in polymeric nanoparticulate systems," *Journal of Photochemistry and Photobiology B: Biology*, Vol. 74, no. 1, pp. 29–38, 2004.

38. Zhang, B., L. Wei, and Z. Chu, "Development of indocyanine green loaded au@ silica core shell nanoparticles for plasmonic enhanced light triggered therapy," *Journal of Photochemistry and Photobiology A: Chemistry*, Vol. 375, pp. 244–251, 2019.

39. Liu, Y., X. Zhi, M. Yang, J. Zhang, L. Lin, X. Zhao, W. Hou, C. Zhang, Q. Zhang, F. Pan, *et al.*, "Tumor-triggered drug release from calcium carbonate-encapsulated gold nanostars for near-infrared photodynamic/photothermal combination antitumor therapy," *Theranostics*, Vol. 7, no. 6, p. 1650, 2017.

40. Moesta, K. T., A. Dmytrijuk, P. M. Schlag, and T. S. Mang, "Individual in-vitro sensitivities of human pancreatic carcinoma cell lines to photodynamic therapy," in *Optical Methods for Tumor Treatment and Detection: Mechanisms and Techniques in Photodynamic Therapy*, Vol. 1645, pp. 43–52, International Society for Optics and Photonics, 1992.

41. Weigand, R., F. Rotermund, and A. Penzkofer, "Aggregation dependent absorption reduction of indocyanine green," *Journal of Physical Chemistry A*, Vol. 101, no. 42, pp. 7729–7734, 1997.